Journal of Global Optimization manuscript No.
(will be inserted by the editor)

Packing Ellipsoids into Volume-Minimizing Rectangular Boxes

Josef Kallrath

Received: date / Accepted: date

Abstract A set of tri-axial ellipsoids, with given semi-axes, is to be packed into a rectangular box; its widths, lengths and height are subject to lower and upper bounds. We want to minimize the volume of this box and seek an overlap-free placement of the ellipsoids which can take any orientation. We present closed non-convex NLP formulations for this ellipsoid packing problem based on purely algebraic approaches to represent rotated and shifted ellipsoids. We consider the elements of the rotation matrix as variables. Separating hyperplanes are constructed to ensure that the ellipsoids do not overlap with each other. For up to 100 ellipsoids we compute feasible points with the global solvers available in GAMS. Only for special cases of two ellipsoids we are able to reach gaps smaller than 10^{-4}.

Keywords Global optimization · non-convex nonlinear programming · packing problem · ellipsoid representation · non-overlap constraints · computational geometry

1 Introduction

Following up on the work by Kallrath (2009, [9]) and Kallrath & Rebennack (2014, [11]; hereafter KR14) we want to pack a set of tri-axial ellipsoids with given semi-axes into one rectangular box limited in size. The ellipsoids can be rotated and be placed freely within that box whose volume should be minimized; from now on, we refer to this problem as *the EPP* to avoid the longer expression *the ellipsoid packing problem*. Ensuring that the ellipsoids do not overlap together with the free rotation of the ellipsoids make this packing problem very difficult. Minimizing the volume of the rectangular box is equivalent to maximizing the packing density ρ.

As in KR14, curiosity partially motivated this work, but then we found also a variety of real world applications, *cf.* Donev et al. (2004a, [5]), Man et al. (2005, [14]) or Uhler & Wright (2013, [19]). Similarly, as in the 2D case for ellipses, ellipsoids can be used a) as an outer approximation or cover, or b) as an inner approximation to approximate irregular or non-convex geometric

J. Kallrath
BASF SE, Scientific Computing, GMC/MS-B009
D-67056 Ludwigshafen, Germany
E-mail: josef.kallrath@web.de

University of Florida, Dept. of Astronomy
Gainesville, FL 32611
E-mail: josef.kallrath@web.de

bodies. From the ellipsoid configurations of a) and b) we can construct feasible points to the original problem and derive bounds on the minimal volume of the rectangular box.

From the point of computational geometry, the problem is also very interesting. For congruent objects, the packing density ρ in ellipsoid packing can exceed that of sphere packing which is bounded by the Kepler conjecture with a value of $\rho = \pi/\sqrt{18} \approx 0.74048$. For congruent ellipsoids we can expect at best densities of the order of 0.75 to 0.78. Densest-known packings of congruent ellipsoids have been found by Donev (2004, [6]). Their family of new ellipsoid configurations consists of crystal arrangements of spheroids with a wide range of aspect ratios (ratio of largest to the smallest semi-axis), and with density ρ always exceeding that of the densest Bravais lattice configurations $\rho = 0.74048$. A remarkable maximum density of $\rho = 0.7707$ is achieved for maximal aspect ratios larger than $\sqrt{3}$, when each ellipsoid has 14 touching neighbors.

A similar problem, packing arbitrary ellipsoids into a master ellipsoid, has been treated by Uhler & Wright (2013, [19]). They minimize the overlap between ellipsoids and use a bi-level optimization formulation, with one algorithm for the general case and another simpler algorithm when all ellipsoids are spheres. Other than this, ellipsoid packing is addressed in physics, where simulation algorithms are used to attack this problem; *cf.* Lubachevsky & Stillinger (1990, [13]) or Donev et al. (2004, [6]).

Our approach starts from a purely algebraic representation of arbitrary tri-axial, rotated ellipsoids to derive a closed NLP formulation. At first, we derive the extreme extensions of shifted and rotated tri-axial ellipsoids. Second, we use the Kuhn-Tucker conditions to derive expressions for the separating hyperplanes to ensure that ellipsoids do not overlap.

This paper contains two contributions. We develop

1. novel mathematical programming models, *i.e.*, closed NLP formulations for the ellipsoid packing problems providing two different approaches to construct the hyperplanes and fitting the ellipsoids into the box,
2. polylithic[1] approaches to construct good and, hopefully, near optimal configurations for larger set of ellipsoids for which the current nonlinear and global solvers do not find feasible points in several hours.

In Sect. 2, we develop NLP models for packing ellipsoids into a rectangular box. We describe polylithic approaches in Sect. 3.3 and present numerical experiments and results in Sect. 3. Sect. 4 concludes the paper.

2 Monolith: non-convex NLP models

We represent ellipsoids by their center coordinates and a rotation matrix to trace their orientation. The two basic blocks of constraints to consider are related (1) to placing the ellipsoids inside the box, and (2) to ensure that ellipsoids do not overlap.

What in KR14 has been said for ellipses in the 2D case, holds also for ellipsoids in the 3D case. Ellipsoids, as they are convex, can be kept apart by separating hyperplanes. We utilize a vector notation in bold symbols using the Euclidean norm scalar products saving the additional dimension index d. Lower case symbols refer to variables, and upper case symbols represent input or derived data. The only exceptions are the semi-axes a_i, b_i, and c_i of the ellipsoids and the model indices. We provide lower and upper bounds on variables as tight as possible to support the global solvers.

We begin with deriving non-overlap and boundary constraints for ellipsoids in Sect. 2.1.

[1] The term *polylithic* has been coined by Kallrath (2009, [8]; 2011, [10]) to refer to tailor-made modeling and solution approaches to solve optimization problems exploiting several models, solve statements in an algebraic modeling language such as GAMS, or algorithms.

To increase computational efficiency, we add symmetry breaking constraints (Sect. 2.5), and lower/upper bounding problems (Sect. 2.6).

2.1 Deriving the NLP model

The objective function minimizes the volume, v, of the rectangular box (prism)

$$\min\ v, \quad v = x_1^{\mathrm{R}} x_2^{\mathrm{R}} x_3^{\mathrm{R}} \quad , \tag{2.1}$$

where x_d^{R} represents the extension of box in dimension d; x_1^{R} denotes the length, x_2^{R} is the width, and x_3^{R} the height of the box.

Equivalently to (2.1), we could minimize waste, *i.e.*,

$$\min\ z, \quad z = v - \sum_{i \in \mathcal{I}} V_i \quad , \tag{2.2}$$

where V_i denotes the volume of ellipsoid i; set $\mathcal{I}$ is the collection of ellipsoids to be packed.

The extensions x_d^{R} of the box are bounded by S_d^- and S_d^+

$$S_d^- \leq x_d^{\mathrm{R}} \leq S_d^+ \quad , \quad \forall d \quad . \tag{2.3}$$

The upper bound, S_d^+, may represent a logistic or technical limitation; a lower bound, S_d^-, is given by the maximum of all the smallest ellipsoidal axes lengths (maximum of $2c_i$ over all i). Improvements S_d^- and S_d^+ are derived in Sect. 2.6 from sphere packings.

2.1.1 Packing spheres

We begin with solving the sphere packing problem for two reasons: first, to compute valid lower and upper bounds on the ellipsoid packing problem (*cf.* Sect. 2.6), and second, to use sphere packing solutions in our polylithic approach (Sect. 3.3).

A necessary and sufficient condition for spheres i and j not to overlap is

$$\left|\mathbf{x}_i^0 - \mathbf{x}_j^0\right|_2^2 := \sum\nolimits_{d=1}^{3} \left(x_{id}^0 - x_{jd}^0\right)^2 \geq (R_i + R_j)^2 \quad , \quad \forall \{ij | i < j\} \quad , \tag{2.4}$$

with radius R_i and the (decision variable) x_{id}^0 representing the center of sphere i in dimension d. Constraints (2.4) are non-convex constraints, as the left hand sides are convex functions. Note that for n spheres lead to $m = n(n-1)/2$ inequalities of type (2.4).

Enclosing the spheres into the box is enforced by

$$x_{id}^0 \geq R_i \quad , \quad \forall \{id\} \qquad \text{and} \qquad x_{id}^0 + R_i \leq x_d^{\mathrm{R}} \quad , \quad \forall \{id\} \quad . \tag{2.5}$$

2.1.2 Packing ellipsoids

Each ellipsoid is characterized by its axes a, b, and c, defining its shape. The ellipsoids can be positioned at the free "center" vector $\mathbf{x}^0$ (with components x_d^0) with semi-axes a, b, and c. Each ellipsoid can be rotated around the three coordinate axes by an angle θ_d. For $\theta_d = 0$, the surface of an ellipsoid is characterized by the equation

$$\frac{(x_1 - x_1^0)^2}{a^2} + \frac{(x_2 - x_2^0)^2}{b^2} + \frac{(x_3 - x_3^0)^2}{c^2} = 1 \quad , \tag{2.6}$$

i.e., all points $(x_1, x_2, x_3) \in \mathbb{R}^3$ satisfying constraint (2.6) are on the surface of the ellipsoid. The rotated ellipsoid is represented by the coordinate transformation

$$\begin{pmatrix} x_1' \\ x_2' \\ x_3' \end{pmatrix} = \mathsf{R} \begin{pmatrix} x_1 - x_1^0 \\ x_2 - x_2^0 \\ x_3 - x_3^0 \end{pmatrix} \quad , \quad \mathsf{R} := \mathsf{R}_3\mathsf{R}_2\mathsf{R}_1$$

with

$$\mathsf{R}_1 := \begin{pmatrix} 1 & 0 & 0 \\ 0 & \cos\theta_1 & -\sin\theta_1 \\ 0 & \sin\theta_1 & \cos\theta_1 \end{pmatrix} \quad , \quad \mathsf{R}_2 := \begin{pmatrix} \cos\theta_2 & 0 & \sin\theta_2 \\ 0 & 1 & 0 \\ -\sin\theta_2 & 0 & \cos\theta_2 \end{pmatrix} \quad ,$$
$$\mathsf{R}_3 := \begin{pmatrix} \cos\theta_3 & -\sin\theta_3 & 0 \\ \sin\theta_3 & \cos\theta_3 & 0 \\ 0 & 0 & 1 \end{pmatrix} \quad . \tag{2.7}$$

R_d, $d \in \mathcal{D}$, describes a rotation around the x_1-axis, x_2-axis and x_3-axis by the Eulerian angles θ_d displayed in Fig. 1; *cf.* Waldron & Schmiedeler (2008, [20]).

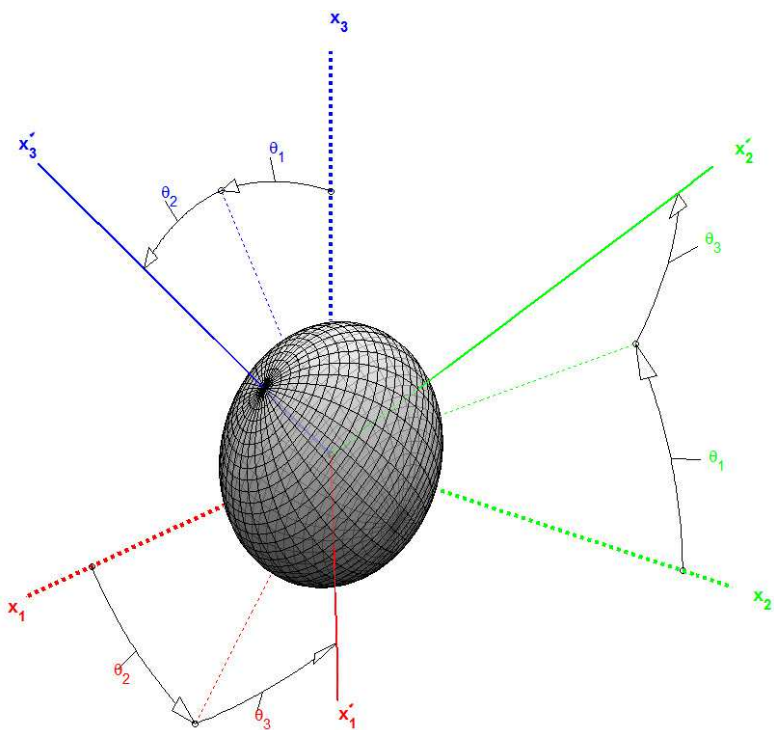

Fig. 1 Ellipsoid rotation: θ_1 represents a rotation of (x_2 and x_3) axis around the x_1- axis, θ_2 represents a rotation of (x_1 and x_3) axis around the x_2- axis and θ_3 represents a rotation of (x_1 and x_2) axis around the x_3- axis.

As some global solver do not support trigonometric terms, we avoid them by using the following transformation leading to an equivalent non-convex, quadratic model. We substitute the decision variable θ_d by the two decision variables

$$v_d := \cos\theta_d \qquad \text{and} \qquad w_d := \sin\theta_d \quad , \quad d \in \mathcal{D} \quad .$$

subject to the bounds $-1 \le v_d \le +1$ and $-1 \le w_d \le +1$ and the Pythagorean theorem

$$v_d^2 + w_d^2 = 1 \quad , \quad d \in \mathcal{D} \quad . \tag{2.8}$$

For ellipsoids, due to their symmetry, it suffices to consider rotation angles, θ_d, in the range of $0°$ to $180°$, *i.e.*, $0 \le w_d \le 1$. With this nomenclature, we obtain the rotation matrices

$$\mathsf{R}_1 := \begin{pmatrix} 1 & 0 & 0 \\ 0 & v_1 & -w_1 \\ 0 & w_1 & v_1 \end{pmatrix}, \quad \mathsf{R}_2 := \begin{pmatrix} v_2 & 0 & w_2 \\ 0 & 1 & 0 \\ -w_2 & 0 & v_2 \end{pmatrix}, \quad \mathsf{R}_3 := \begin{pmatrix} v_3 & -w_3 & 0 \\ w_3 & v_3 & 0 \\ 0 & 0 & 1 \end{pmatrix} \quad ,$$

and thus

$$\mathsf{R} = \mathsf{R}_3\mathsf{R}_2\mathsf{R}_1 = \begin{pmatrix} v_2v_3 & -v_1w_3 + w_1v_3w_2 & w_1w_3 + v_1v_3w_2 \\ v_2w_3 & v_1v_3 + w_1w_2w_3 & -w_1v_3 + v_1w_2w_3 \\ -w_2 & v_2w_1 & v_1v_2 \end{pmatrix} \tag{2.9}$$

Let us now represent the surface of an arbitrarily oriented ellipsoid, centered at $\mathbf{x}^0 \in \mathbb{R}^3$ by the quadratic form

$$(\mathbf{x} - \mathbf{x}^0)^\top \mathsf{A}(\mathbf{x} - \mathbf{x}^0) = 1 \quad , \mathbf{x} \in \mathbb{R}^3 \quad , \tag{2.10}$$

where A is a positive definite matrix.

The eigenvectors of A are the principal directions of the ellipsoid axes in 3-D and the eigenvalues of A are the reciprocal squares of the lengths of semi-axes a^{-2}, b^{-2} and c^{-2}. An invertible linear transformation applied to a sphere produces an ellipsoid, which can be transformed to the standard form (2.10) by a suitable rotation R. For an ellipsoid with semi-axes a, b and c rotated by R as defined in (2.9), we obtain

$$\mathsf{A} := \mathsf{R}\mathsf{D}\mathsf{R}^\top = \mathsf{R}_3\mathsf{R}_2\mathsf{R}_1\mathsf{D}\mathsf{R}_1^\top\mathsf{R}_2^\top\mathsf{R}_3^\top, \quad \mathsf{D} := \begin{pmatrix} \lambda_1 & 0 & 0 \\ 0 & \lambda_2 & 0 \\ 0 & 0 & \lambda_3 \end{pmatrix} = \begin{pmatrix} a & 0 & 0 \\ 0 & b & 0 \\ 0 & 0 & c \end{pmatrix}^{-2} \quad ,$$

and the matrices R_d as defined in (2.7). The transposed matrices $\mathsf{R}_d^\top$ are

$$\mathsf{R}_1^\top := \begin{pmatrix} 1 & 0 & 0 \\ 0 & v_1 & w_1 \\ 0 & -w_1 & v_1 \end{pmatrix}, \quad \mathsf{R}_2^\top := \begin{pmatrix} v_2 & 0 & -w_2 \\ 0 & 1 & 0 \\ w_2 & 0 & v_2 \end{pmatrix}, \quad \mathsf{R}_3^\top := \begin{pmatrix} v_3 & w_3 & 0 \\ -w_3 & v_3 & 0 \\ 0 & 0 & 1 \end{pmatrix} \quad .$$

Thus we obtain for A polynomial expressions up to degree six

$$\begin{aligned}
A_{11} &= -2v_1w_1v_3w_2w_3\lambda_2 + 2v_1w_1v_3w_2w_3\lambda_3 \\
&\quad + v_2^2v_3^2\lambda_1 + v_1^2w_3^2\lambda_2 + w_1^2w_3^2\lambda_3 + v_1^2v_3^2w_2^2\lambda_3 + w_1^2v_3^2w_2^2\lambda_2 \\
A_{12} &= -v_1^2v_3w_3\lambda_2 + v_2^2v_3w_3\lambda_1 - w_1^2v_3w_3\lambda_3 + v_1w_1v_3^2w_2\lambda_2 - v_1w_1w_2w_3^2\lambda_2 \\
&\quad - v_1w_1v_3^2w_2\lambda_3 + v_1w_1w_2w_3^2\lambda_3 + v_1^2v_3w_2^2w_3\lambda_3 + w_1^2v_3w_2^2w_3\lambda_2 \\
A_{13} &= -v_2v_3w_2\lambda_1 - v_1v_2w_1w_3\lambda_2 + v_1v_2w_1w_3\lambda_3 + v_2w_1^2v_3w_2\lambda_2 + v_1^2v_2v_3w_2\lambda_3 \\
A_{22} &= 2v_1w_1v_3w_2w_3\lambda_2 - 2v_1w_1v_3w_2w_3\lambda_3 + v_1^2v_3^2\lambda_2 + v_2^2w_3^2\lambda_1 + w_1^2v_3^2\lambda_3 \\
&\quad + v_1^2w_2^2w_3^2\lambda_3 + w_1^2w_2^2w_3^2\lambda_2 \\
A_{23} &= -v_2w_2w_3\lambda_1 + v_1v_2w_1v_3\lambda_2 - v_1v_2w_1v_3\lambda_3 + v_2w_1^2w_2w_3\lambda_2 + v_1^2v_2w_2w_3\lambda_3 \\
A_{33} &= w_2^2\lambda_1 + v_1^2v_2^2\lambda_3 + v_2^2w_1^2\lambda_2 \quad .
\end{aligned}$$

Due to the symmetry of A, *i.e.*, $\mathsf{A}^\top = \mathsf{A}$, we can add

$$A_{21} = A_{12} \quad , \quad A_{31} = A_{13} \quad , \quad A_{32} = A_{23} \quad . \tag{2.11}$$

Given all the multi-linear terms, we suggest a different route and approach: Take

$$\mathsf{R} = \begin{pmatrix} R_{11} & R_{12} & R_{13} \\ R_{21} & R_{22} & R_{23} \\ R_{31} & R_{32} & R_{33} \end{pmatrix}$$

as the fundamental variables instead of the 3 Eulerian angles; we drop the index i referring to a specific ellipsoid. R is an rotation matrix, if and only if $\mathsf{R}^{-1} = \mathsf{R}^\top$ and $\det\mathsf{R} = 1$. This we need to guarantee by 6+1 equations: the orthonormality established by the scalar products of row m ($\mathbf{r}_m$) and column n ($\mathbf{r}_n$) of R

$$\mathbf{r}_m^\top \mathbf{r}_n = \delta_{mn} \quad , \quad \forall \{mn | m \geq n\} \quad , \tag{2.12}$$

and to exclude reflections by

$$\begin{aligned} 1 = \det \mathsf{R} = & R_{11}R_{22}R_{33} - R_{11}R_{23}R_{32} - R_{12}R_{21}R_{33} \\ & + R_{12}R_{31}R_{23} + R_{21}R_{13}R_{32} - R_{13}R_{22}R_{31} \quad . \end{aligned} \tag{2.13}$$

We could also look at R as a unitary matrix, the most general form of rotation in a vector space over complex numbers of any dimensions, and widely used in Quantum Mechanics; *cf.* Dirac (1974, [4]). In a metric space the unitary transformations preserve the scalar product (hence the length of all vectors and their angles) and the parity (number of inverted base vectors cannot be odd) which is the essence of rotation, *cf.* Halmos (1974, [7]).

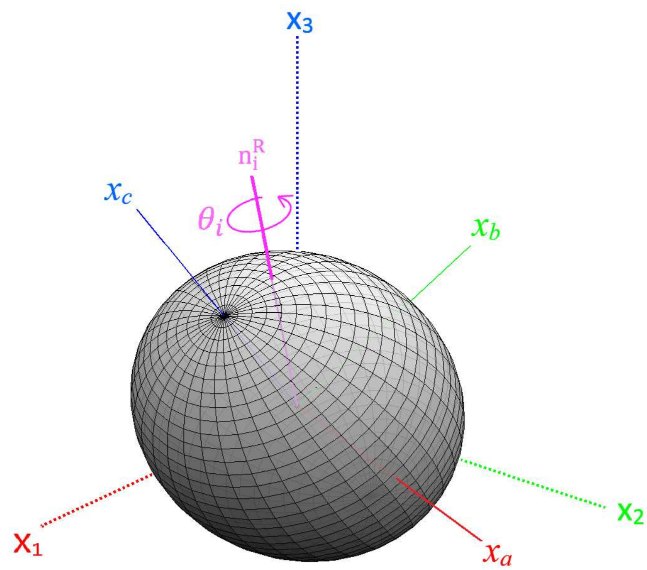

Fig. 2 Ellipsoid rotation: θ_i represents a rotation around the $\mathbf{n}_i^{\mathrm{R}}$-axis. The axes x_a, x_b and x_c are parallel to the semi-axes of the ellipsoids, while x_1, x_2 and x_3 are the coordinate axes of the un-rotated coordinate system.

We also implemented a third approach to deal with R, which starts from one rotation axis, $\mathbf{n}_i^{\mathrm{R}}$, and one rotation angle θ_i for each ellipsoid as displayed in Fig. 2, and compute R as a function of the unit vector $\mathbf{n}_i^{\mathrm{R}}$ and θ_i according to

$$\mathsf{R}_i = \mathsf{B}_i \begin{pmatrix} \cos\theta_i & -\sin\theta_i & 0 \\ \sin\theta_i & \cos\theta_i & 0 \\ 0 & 0 & 1 \end{pmatrix} \mathsf{B}_i^{\mathrm{T}} \quad ,$$

where the third column, B_{i3}, of B_i is $\mathbf{n}_i^{\mathrm{R}}$. The first and the second column, B_{i1} and B_{i2}, of B_i need to be computed in such a way that they three columns of B_i form a right-handed orthonormal system, *i.e.*, $\mathsf{B}_i\mathsf{B}_i^{\mathrm{T}} = \mathbb{1}$. This is established by the cross product

$$\mathsf{B}_{i3} = \mathsf{B}_{i1} \times \mathsf{B}_{i2} \tag{2.14}$$

and the determinant condition

$$\det \mathsf{B}_i = 1 \quad , \quad \forall \{i\} \quad . \tag{2.15}$$

The nine elements of B_i are treated as variables.

Thus, in total, we have three approaches how to treat R (we neglect the index i for each ellipsoid):

- R1: The nine elements of R are declared as variables subject to $\det \mathsf{R} = 1$ and the orthonormality condition $\mathsf{B}_i\mathsf{B}_i^{\mathrm{T}} = \mathbb{1}$. This approach works best to find feasible solutions quickly.
- R2: The nine elements of R are declared as variables subject to expression which relate them to the Eulerian angles. The problem is that the Eulerian angles are not unique.
- R3: The nine elements of R are declared as variables subject to (2.14) and (2.15). This approach does not suffer from uniqueness problems related to the Eulerian angles, but the increased number of variables is not helpful.

Note that the approaches R2 and R3 are just special cases of R1 where the coefficients are expressed as functions of angles, be it the Eulerian angles or just one angle around one axis. Independent of which approach we use to treat R, we take

$$\mathsf{A} = \mathsf{R}\mathsf{D}\mathsf{R}^{\top}$$

which leads to

$$\mathsf{A} = \begin{pmatrix} R_{11} & R_{12} & R_{13} \\ R_{21} & R_{22} & R_{23} \\ R_{31} & R_{32} & R_{33} \end{pmatrix} \begin{pmatrix} \lambda_1 & 0 & 0 \\ 0 & \lambda_2 & 0 \\ 0 & 0 & \lambda_3 \end{pmatrix} \begin{pmatrix} R_{11} & R_{21} & R_{31} \\ R_{12} & R_{22} & R_{32} \\ R_{13} & R_{23} & R_{33} \end{pmatrix}$$

which results in

$$\begin{aligned}
A_{11} &= R_{11}^2\lambda_1 + R_{12}^2\lambda_2 + R_{13}^2\lambda_3 \\
&= -2v_1w_1v_3w_2w_3\lambda_2 + 2v_1w_1v_3w_2w_3\lambda_3 \\
&\quad + v_2^2v_3^2\lambda_1 + v_1^2w_3^2\lambda_2 + w_1^2w_3^2\lambda_3 + v_1^2v_3^2w_2^2\lambda_3 + w_1^2v_3^2w_2^2\lambda_2 \\
A_{12} &= R_{11}R_{21}\lambda_1 + R_{12}R_{22}\lambda_2 + R_{13}R_{23}\lambda_3 \\
&= -v_1^2v_3w_3\lambda_2 + v_2^2v_3w_3\lambda_1 - w_1^2v_3w_3\lambda_3 + v_1w_1v_3^2w_2\lambda_2 - v_1w_1w_2w_3^2\lambda_2 \\
&\quad - v_1w_1v_3^2w_2\lambda_3 + v_1w_1w_2w_3^2\lambda_3 + v_1^2v_3w_2^2w_3\lambda_3 + w_1^2v_3w_2^2w_3\lambda_2 \\
A_{13} &= R_{11}R_{31}\lambda_1 + R_{12}R_{32}\lambda_2 + R_{13}R_{33}\lambda_3 \\
&= -v_2v_3w_2\lambda_1 - v_1v_2w_1w_3\lambda_2 + v_1v_2w_1w_3\lambda_3 + v_2w_1^2v_3w_2\lambda_2 + v_1^2v_2v_3w_2\lambda_3 \\
A_{22} &= R_{21}^2\lambda_1 + R_{22}^2\lambda_2 + R_{23}^2\lambda_3 \\
&= 2v_1w_1v_3w_2w_3\lambda_2 - 2v_1w_1v_3w_2w_3\lambda_3 + v_1^2v_3^2\lambda_2 + v_2^2w_3^2\lambda_1 + w_1^2v_3^2\lambda_3 \\
&\quad + v_1^2w_2^2w_3^2\lambda_3 + w_1^2w_2^2w_3^2\lambda_2 \\
A_{23} &= R_{21}R_{31}\lambda_1 + R_{22}R_{32}\lambda_2 + R_{23}R_{33}\lambda_3 \\
&= -v_2w_2w_3\lambda_1 + v_1v_2w_1v_3\lambda_2 - v_1v_2w_1v_3\lambda_3 + v_2w_1^2w_2w_3\lambda_2 + v_1^2v_2w_2w_3\lambda_3 \\
A_{33} &= R_{31}^2\lambda_1 + R_{32}^2\lambda_2 + R_{33}^2\lambda_3 = w_2^2\lambda_1 + v_1^2v_2^2\lambda_3 + v_2^2w_1^2\lambda_2 \quad .
\end{aligned} \tag{2.16}$$

or, in short

$$A_{mn} = \sum_{d\in\mathcal{D}} R_{md}R_{nd}\lambda_d \quad , \quad \forall\{(mn)|m\in\mathcal{D}, n\in\mathcal{D}\} \quad ,$$

and thus, again the symmetry

$$\mathsf{A}^\top = \mathsf{A} \quad .$$

To support the global solver with bounds on the variables, it is also useful to note that

$$|A_{mn}| \leq \sum_{d\in\mathcal{D}} |R_{md}R_{nd}\lambda_d| \leq \sum_{d\in\mathcal{D}} \lambda_d \quad , \quad \forall\{(mn)|m\in\mathcal{D}, n\in\mathcal{D}\} \quad . \tag{2.17}$$

All bilinear terms $R_{jk}R_{mn}$ are already used in (2.12). Therefore, we introduce auxiliary variables u_{jkmn} exploiting that $u_{jkmn} = u_{mnjk}$, *i.e.*, we consider only those tuples with $j \leq m$ and $k \leq n$, which leads to $3 + \frac{3^4-3}{2} = 42$ variables for each ellipsoid. Note that A is linear in u_{jkmn}. Unfortunately, the computation of $\det \mathsf{R}$ does not benefit from u_{jkmn} as those terms do not show up before.

Knowing A_i and the origin $\mathbf{x}_i^0$ of ellipsoid i, we plot the ellipsoids as described in Appendix B.4.

2.2 Exploiting A to fit overlap-free ellipsoids into the box

We start with explicit approaches, exploiting A to fit the ellipsoids into the box and to ensure that they do not overlap. Later, we develop an alternative approach not resorting to A.

2.2.1 Minimum and maximum extensions of ellipsoids

To fit the ellipsoids inside the enclosing box, we proceed exactly as in KR14 and require that

$$0 \leq x_{id}^- \leq x_{id}^+ \leq x_d^{\mathrm{R}} \quad , \quad \forall\{id\} \quad , \tag{2.18}$$

where the extreme extensions, x_{id}^- and x_{id}^+, of ellipsoid i in dimension d with center x_{id}^0 follow from the optimization problems

$$\begin{aligned} x_{id}^- &= \min\ \mathbf{c}^\top\mathbf{x} = \min\ x_{id} \quad , \quad \forall d \qquad \text{and} \\ x_{id}^+ &= \max\ \mathbf{c}^\top\mathbf{x} = \max\ x_{id} \quad , \quad \forall d \quad , \end{aligned}$$

respectively, subject to the ellipsoid condition (2.10). As shown in Appendix B.2, the minimal and maximal extensions of the ellipsoid in the first dimension, ($d = 1$), are given by

$$x_1^- = \min\ \mathbf{c}^\top(\mathbf{x}+\mathbf{x}^0) = x_1^0 - abc\sqrt{A_{22}A_{33} - A_{23}A_{32}} \tag{2.19}$$

and

$$x_1^+ = \max\ \mathbf{c}^\top(\mathbf{x}+\mathbf{x}^0) = x_1^0 + abc\sqrt{A_{22}A_{33} - A_{23}A_{32}} \quad , \tag{2.20}$$

respectively. Note that these formulae are similar to (18) and (19) KR14 obtained for the maximal extensions of ellipsoids (2D case). If the ellipsoids were spheres ($a = b = c = r$), for $\theta_1 = \theta_2 = \theta_3 = 0$, we obtain $x_1^+ = x_1^0 + abc\sqrt{b^{-2}c^{-2} - 0} = x_1^0 + r$.

Similarly, for $d = 2$ we obtain in Appendix B.2

$$x_2^- = x_2^0 - abc\sqrt{A_{11}A_{33} - A_{13}A_{31}} \tag{2.21}$$

$$x_2^+ = x_2^0 + abc\sqrt{A_{11}A_{33} - A_{13}A_{31}} \quad . \tag{2.22}$$

Finally, the minimum and maximum extensions of ellipsoid i in the third dimension, $(d = 3)$, are given by

$$x_3^- = x_3^0 - abc\sqrt{A_{11}A_{22} - A_{12}A_{21}} \tag{2.23}$$

$$x_3^+ = x_3^0 + abc\sqrt{A_{11}A_{22} - A_{12}A_{21}} \quad . \tag{2.24}$$

These constraints are complemented by

$$x_{id}^0 \geq c_i \quad , \quad \forall\{id\} \qquad \text{and} \qquad x_{id}^0 + c_i \leq x_d^{\mathrm{R}} \quad , \quad \forall\{id\} \quad . \tag{2.25}$$

2.2.2 Non-overlap conditions for ellipsoids

One could separate ellipsoids based on the Eigenvalue approach by Choi et al. (2009,[3]), which exploits the roots of

$$f(\lambda) = \det(\lambda \mathsf{A}_i - \mathsf{A}_j)$$

and the following theorems: Ellipsoids i and j are detached if and only if $f(\lambda) = 0$ has two different negative roots. Ellipsoids i and j touch each other in one point if and only if $f(\lambda) = 0$ has a negative double root. We do not follow this approach, as it seems to us to be too complicated to implement the eigenvalue computation and the two-different-root condition in an NLP model.

Another techniques to deal with non-overlap conditions in cutting or packing problems is the phi-function approach; *cf* Chernov et al. (2012,[2] for 2D cutting and packing problems, Stoyan &Chugay (2008, [17]) for solving 3D packing problems, or Romanova et al. (2011, [16]) for covering problems. However, in this approach, only local optimality can be proven and it is not clear how this approach could be translated into a declarative NLP model.

Instead of these two approach mentioned above, we use the following explicit separating hyperplanes approach illustrated in Fig. 3. The column vector $\mathbf{c}$ in (B.72), (B.73) or, (B.76) will be selected as the normal vector $\mathbf{n}_{ij}^{\mathrm{H}}$ of the separating plane H_{ij}. Then $\mathbf{c}^\top \mathbf{x}$ measures the maximal extension of the ellipsoid in the direction to the separating plane. Therefore, for the moment, we consider $\mathbf{c}$ as a general vector. Although, we cannot solve the resulting Karush-Kuhn-Tucker (KKT) conditions analytically, we safe ourselves the trouble of going through all the geometry. Our idea is: Let $d_{ij}^{C\mathrm{i}}$ denote the distance of the origin $\mathbf{x}_i^0$ of ellipsoid i from H_{ij} defined by $\mathbf{n}_{ij}^{\mathrm{H}}\mathbf{x} = d_{ij}^{\mathrm{H}}$, *i.e.*, we assume that H_{ij} is given. In this context, we also assume that $\mathbf{x}_i^0$ is known. Note that as we assume $a \geq b \geq c$, the smallest semi-axis, c, of ellipsoid i provides a lower bound on $d_{ij}^{C\mathrm{i}}$.

We want to minimize the distance, $d_{ij}^{0\mathrm{i}}$, of ellipsoid i to H_{ij}, *i.e.*,

$$\begin{aligned} d_{ij}^{0\mathrm{i}} &= \min\left\{\mathbf{c}^\top(\mathbf{x} + \mathbf{x}_i^0) - d_{ij}^{\mathrm{H}}\right\} \\ &= \mathbf{n}_{ij}^{\mathrm{H}}(\mathbf{x}_{ij}^{\mathrm{i}} + \mathbf{x}_i^0) - d_{ij}^{\mathrm{H}} = \mathbf{n}_{ij}^{\mathrm{H}}\mathbf{x}_{ij}^{\mathrm{i}} + \mathbf{n}_{ij}^{\mathrm{H}}\mathbf{x}_i^0 - d_{ij}^{\mathrm{H}} = \mathbf{n}_{ij}^{\mathrm{H}}\mathbf{x}_{ij}^{\mathrm{i}} + d_{ij}^{C\mathrm{i}} \end{aligned} \tag{2.26}$$

with $\mathbf{c}^\top = \mathbf{n}_{ij}^{\mathrm{H}}$ subject to (B.74) and

$$d_{ij}^{C\mathrm{i}} = \mathbf{n}_{ij}^{\mathrm{H}}\mathbf{x}_i^0 - d_{ij}^{\mathrm{H}} \quad . \tag{2.27}$$

Note that distance $d_{ij}^{0\mathrm{i}}$ can be positive or negative, or zero if the ellipsoid touches H_{ij}. If ellipsoid i is located on *that* side or half-space of H_{ij} into which the normal vector $\mathbf{n}_{ij}^{\mathrm{H}}$ points, we have $d_{ij}^{0\mathrm{i}} \geq 0$. Therefore, we label the ellipsoids consistently with the request

$$d_{ij}^{C\mathrm{i}} > d_{ij}^{0\mathrm{i}} \geq 0 \wedge d_{ij}^{C\mathrm{j}} < d_{ij}^{0\mathrm{j}} \leq 0 \quad . \tag{2.28}$$

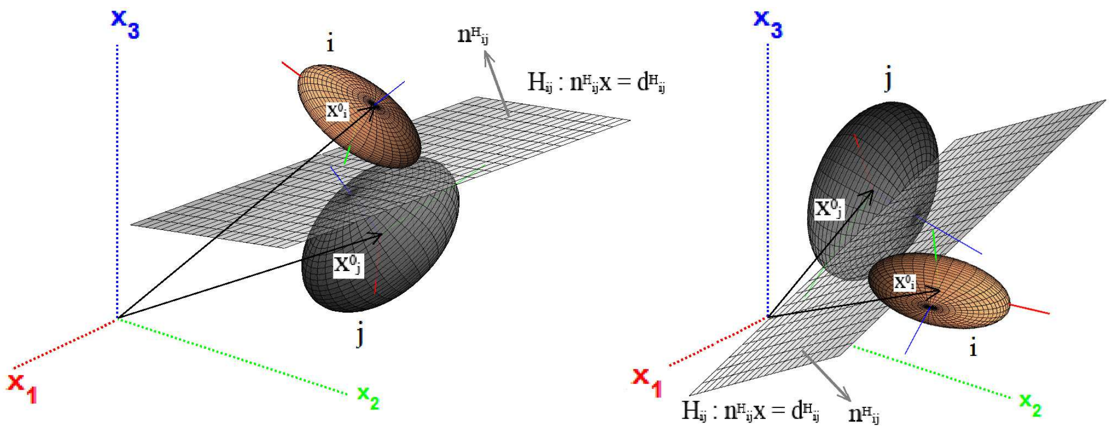

Fig. 3 Ellipsoids and the separating plane H_{ij}.

The chain (2.28) of inequalities is useful to separate the points of minimal and maximal distance of ellipsoid to H_{ij}.

Let us now compute the minimal distances by exploiting the Lagrangian function

$$\mathcal{L}(\mathbf{x},\bar{\lambda}) = \mathbf{c}^\top(\mathbf{x}+\mathbf{x}_i^0) - d_{ij}^{\mathrm{H}} + \bar{\lambda}_{ij}^{\mathrm{i}}\left(\mathbf{x}^\top \mathsf{A}_i \mathbf{x} - 1\right) \quad .$$

The first-order KKT conditions are derived as

$$\mathbf{c} + 2\bar{\lambda}_{ij}^{\mathrm{i}} \mathsf{A}_i^\top \mathbf{x} = \mathbf{0} \tag{2.29}$$

together with the point-on-ellipsoid condition (2.10)

$$\mathbf{x}^\top \mathsf{A}_i \mathbf{x} = 1 \quad .$$

Let us denote the extreme points satisfying (2.29) and (2.10) by $\mathbf{x}^{\mathrm{i}}$ or $\mathbf{x}_{ij}^{\mathrm{i}}$, respectively. Similarly, we need to establish the KKT conditions for ellipsoid j leading to $\bar{\lambda}_{ij}^{\mathrm{i}}$, $\mathbf{x}^{\mathrm{j}}$, and $\mathbf{x}_{ij}^{\mathrm{j}}$.

To solve the trilinear equations (2.29) and (2.10) and to reduce them to bilinear terms, we introduce the auxiliary vector $\mathbf{y}_{ij}^{\mathrm{j}}$

$$\mathbf{y}_{ij}^{\mathrm{i}} = \mathsf{A}_i \mathbf{x}_{ij}^{\mathrm{i}} \quad , \tag{2.30}$$

and insert it in $\mathbf{x}^\top \mathsf{A}_i \mathbf{x} = 1$

$$\mathbf{x}_{ij}^{\mathrm{i}\top} \mathbf{y}_{ij}^{\mathrm{i}} = 1 \quad ,$$

and in (2.29)

$$\mathbf{c} + 2\bar{\lambda}_{ij}^{\mathrm{i}} \mathbf{y}_{ij}^{\mathrm{i}} = \mathbf{n}_{ij}^{\mathrm{H}} + 2\bar{\lambda}_{ij}^{\mathrm{i}} \mathbf{y}_{ij}^{\mathrm{i}} = \mathbf{0} \quad , \tag{2.31}$$

where we have exploited that A is symmetric. Thus, the problem is reduced to three bilinear equations. Alternatively, if we were interested in fewer constraints, we could proceed as follows. We left-multiply (2.29) by $\mathbf{x}^\top \neq \mathbf{0}$, (this multiplication does not cause problems, because $\mathbf{0}$ cannot be an extreme point of the problem at hand) and exploit (B.74) to obtain $\mathbf{x}^\top \mathbf{c} + 2\bar{\lambda} = 0$, which enables us to eliminate the Lagrangian multiplier $\bar{\lambda}$ from (2.29) yielding

$$\mathbf{c} - (\mathbf{x}^\top \mathbf{c}) \mathsf{A}_i^\top \mathbf{x} = \mathbf{n}_{ij}^{\mathrm{H}} - (\mathbf{x}^\top \mathbf{n}_{ij}^{\mathrm{H}}) \mathsf{A}_i^\top \mathbf{x} = 0 \quad . \tag{2.32}$$

or, to be precise

$$\mathbf{n}_{ij}^{\mathrm{H}} - (\mathbf{x}_{ij}^{\mathrm{i}\top} \mathbf{n}_{ij}^{\mathrm{H}}) \mathsf{A}_i^\top \mathbf{x}_{ij}^{\mathrm{i}} = 0 \quad . \tag{2.33}$$

As there exist two extreme points $\tilde{\mathbf{x}}_{ij}^{\mathrm{i}}$ with a maximal and a minimal distance to the separating plane H_{ij}, we need to separate them, or to work with a sufficient condition of our minimization problem. Fortunately, the minimal extreme points are selected by applying (2.28). The maximal distance points is further away from H_{ij} than the center of the ellipsoid, which in turn is further away than the minimal point. Thus, we need just to add the computation of the center-of-ellipsoid distance (2.27) and the distance of the ellipsoid according to (2.26).

Let n denote the number of ellipsoids, $D = 3$ the number of dimensions, and $m = n(n-1)/2$, then we obtain Table 1 for the number of constraints and variables.

Table 1 Number, N_{var}, of variables and number, N_{con}, constraints for non-overlap conditions for ellipsoids

Equations	**variables**	N_{var}	N_{con}
1) minimum distance of ellipsoid i to H_{ij}, (2.26)	$d_{ij}^{0\mathrm{i}}, d_{ij}^{\mathrm{Ci}}, n_{ij}^{\mathrm{H}}$	$D \times (m + 2 \times n)$	$D \times n$
2) center-of-ellipsoid distance to H_{ij}, (2.27)	$d_{ij}^{\mathrm{H}}, (n_{ij}^{\mathrm{H}}, d_{ij}^{\mathrm{Ci}})$	$D \times m$	$D \times n$
3) minimal & maximal distance of ellipsoid i to H_{ij}, (2.28)	$(d_{ij}^{0\mathrm{i}}, d_{ij}^{\mathrm{Ci}}, d_{ij}^{0\mathrm{j}}, d_{ij}^{\mathrm{Cj}})$	-	$D \times m$
4) auxiliary vector y_{ij}^{i} for ellipsoid i, (2.30)	y_{ij}^{i}	$D \times n$	$D \times n$
5) bilinear form of (2.29) for ellipsoid i, (2.31)	$(n_{ij}^{\mathrm{H}}, y_{ij}^{\mathrm{i}})$	-	$D \times n$

2.3 Half-space approach

As the number of the variables and constraints increases quadratically in n, we construct an additional, rather implicit approach to ensure that two ellipsoids i and j, $i < j$, do not overlap. If we describe each ellipsoid with center $\mathbf{x}^0$ as an affine transformation of the unit sphere

$$\mathcal{E} := \left\{ \mathbf{x}^0 + L\mathbf{u} \;\mid\; \|\mathbf{u}\|_2 \;\leq\; 1 \right\} \quad , \quad \mathsf{L} = \mathsf{R}\Lambda \quad , \quad \Lambda := \operatorname{diag}(a, b, c) \tag{2.34}$$

with a 3 x 3 matrix L and a vector $\mathbf{u} \in \mathbb{R}$, non overlap is ensured by

$$\mathbf{n}_{ij}^{\mathrm{H}} \left(\mathbf{x}_j^0 - \mathbf{x}_i^0 \right) \geq \left\| \mathsf{L}_i \mathbf{n}_{ij}^{\mathrm{H}} \right\|_2 + \left\| \mathsf{L}_j \mathbf{n}_{ij}^{\mathrm{H}} \right\|_2 \quad . \tag{2.35}$$

Proof: The separating hyperplane

$$H_{ij} : \mathbf{n}_{ij}^{\mathrm{H}} \mathbf{x} = d_{ij}^{\mathrm{H}}$$

with normal vector, $\mathbf{n}_{ij}^{\mathrm{H}} \neq \mathbf{0}$, and distance, d_{ij}^{H}, to the origin of the coordinate system defines a half-space

$$\mathcal{H}_{ij}^{+} := \left\{ \mathbf{x} | \mathbf{n}_{ij}^{\mathrm{H}} \mathbf{x} \leq d_{ij}^{\mathrm{H}} \right\} \quad .$$

For simplicity, let us start with a unit sphere centered at the origin of the coordinate system and derive a condition for H_{ij} such that the unit sphere

$$\mathcal{S} := \{ \mathbf{x} \,|\, \|\mathbf{x}\|_2 \leq 1 \}$$

is fully contained in half-space H_{ij}^{+}. The half-space condition $\mathbf{n}_{ij}^{\mathrm{H}} \mathbf{x} \leq d_{ij}^{\mathrm{H}}$ is equivalent to

$$d_{ij}^{\mathrm{H}} \geq \max_{\mathbf{x} \in \mathcal{S}} \mathbf{n}_{ij}^{\mathrm{H}} \mathbf{x} \quad .$$

Geometrically, the maximal value of $\mathbf{n}_{ij}^{\mathrm{H}}\mathbf{x}$ is obtained when $\mathbf{n}_{ij}^{\mathrm{H}}$ and $\mathbf{x}$ are parallel. Formally, we could compute the maximum by applying the Cauchy-Schwartz inequality, *i.e.*,

$$\mathbf{n}_{ij}^{\mathrm{H}}\mathbf{x} \leq \left\|\mathbf{n}_{ij}^{\mathrm{H}}\right\|_2 \|\mathbf{x}\|_2 \leq \left\|\mathbf{n}_{ij}^{\mathrm{H}}\right\|_2 \quad .$$

Therefore, the condition is

$$d_{ij}^{\mathrm{H}} \geq \left\|\mathbf{n}_{ij}^{\mathrm{H}}\right\|_2 \quad .$$

If the plane's normal vector is normalized to unity, $\left\|\mathbf{n}_{ij}^{\mathrm{H}}\right\|_2 = 1$, we get

$$d_{ij}^{\mathrm{H}} \geq 1 \quad ,$$

i.e., independent on the orientation of the plane H_{ij}, it just needs to have a distance of at least one to have $\mathcal{S}$ in the half-space specified.

If we now consider an ellipsoid centered at an arbitrary origin $\mathbf{x}^0$ using its representation

$$\mathcal{E} := \left\{\mathbf{x}^0 + L\mathbf{u} \ \mid\ \|\mathbf{u}\|_2 \ \leq\ 1\right\} \quad , \quad \mathsf{L} = \mathsf{R}\Lambda$$

with a combined rotation-shape matrix L, we can derive a similar condition for the parameters $(\mathbf{n}_{ij}^{\mathrm{H}}, d_{ij}^{\mathrm{H}})$ describing hyperplane H_{ij} so that $\mathcal{E}$ is fully contained in $\mathcal{H}_{ij}^{+}$. The containment condition $\mathcal{H}_{ij}^{+} \supseteq \mathcal{E}$ now becomes

$$d_{ij}^{\mathrm{H}} \geq \max_{\mathbf{u}\in\mathcal{S}} \mathbf{n}_{ij}^{\mathrm{H}}\left(\mathbf{x}^0 + L\mathbf{u}\right) = \mathbf{n}_{ij}^{\mathrm{H}}\mathbf{x}^0 + \max_{\mathbf{u}\in\mathcal{S}} L\mathbf{u} = \mathbf{n}_{ij}^{\mathrm{H}}\mathbf{x}^0 + \left\|\mathsf{L}\mathbf{n}_{ij}^{\mathrm{H}}\right\|_2 \quad ,$$

where we have used the same argument and the Cauchy-Schwartz inequality as for the unit sphere case. If we want to confine $\mathcal{E}$ to the other half-space $\mathcal{H}_{ij}^{-}$

$$\mathcal{H}_{ij}^{-} := \left\{\mathbf{x} | \mathbf{n}_{ij}^{\mathrm{H}}\mathbf{x} \geq d_{ij}^{\mathrm{H}}\right\}$$

of hyperplane H_{ij}, we just replace $(\mathbf{n}_{ij}^{\mathrm{H}}, d_{ij}^{\mathrm{H}})$ by $-(\mathbf{n}_{ij}^{\mathrm{H}}, d_{ij}^{\mathrm{H}})$, and obtain

$$d_{ij}^{\mathrm{H}} \leq \mathbf{n}_{ij}^{\mathrm{H}}\mathbf{x}^0 - \left\|\mathsf{L}^{\mathrm{T}}\mathbf{n}_{ij}^{\mathrm{H}}\right\|_2 \quad .$$

If we now consider two ellipsoids $\mathcal{E}_i$ and $\mathcal{E}_j$, we conclude that hyperplane H_{ij} separates $\mathcal{E}_i$ and $\mathcal{E}_j$, *i.e.*, keeps them on different sides, if

$$\mathbf{n}_{ij}^{\mathrm{H}}\mathbf{x}_i^0 + \left\|\mathsf{L}_i^{\mathrm{T}}\mathbf{n}_{ij}^{\mathrm{H}}\right\|_2 \leq d_{ij}^{\mathrm{H}} \leq \mathbf{n}_{ij}^{\mathrm{H}}\mathbf{x}_j^0 - \left\|\mathsf{L}_j^{\mathrm{T}}\mathbf{n}_{ij}^{\mathrm{H}}\right\|_2 \quad ,$$

which is equivalent to

$$\mathbf{n}_{ij}^{\mathrm{H}}\left(\mathbf{x}_j^0 - \mathbf{x}_i^0\right) \geq \left\|\mathsf{L}_i\mathbf{n}_{ij}^{\mathrm{H}}\right\|_2 + \left\|\mathsf{L}_j\mathbf{n}_{ij}^{\mathrm{H}}\right\|_2 \quad . \tag{2.36}$$

Note that using (2.35) non-overlap is ensured by only m inequalities involving two square root functions and quadrilinear terms, and additionally m equalities to ensure that the normal vector $\mathbf{n}_{ij}^{\mathrm{H}}$ is a unit vector, *i.e.*,

$$\left\|\mathbf{n}_{ij}^{\mathrm{H}}\right\|_2 = 1 \quad \Leftrightarrow \quad \sum_d \left(n_{ijd}^{\mathrm{H}}\right)^2 = 1 \quad , \quad \forall\{ij|i<j\} \quad . \tag{2.37}$$

The normalization (2.37) is not necessary as such, but somehow we need to ensure that $\mathbf{n}_{ij}^{\mathrm{H}} \neq \mathbf{0}$, as (2.36) would be trivially fulfilled by $\mathbf{n}_{ij}^{\mathrm{H}} = \mathbf{0}$. Let us give some interpretation of (2.36) by considering two ellipsoids with $R_i = a_i = b_i = c_i$ and $R_j = a_j = b_j = c_j$, *i.e.*, two spheres. For spheres, we have $\mathbf{n}_{ij}^{\mathrm{H}} = \pm\left(\mathbf{x}_j^0 - \mathbf{x}_i^0\right)$. In the special case that both spheres touch each other, we obtain

$$\begin{aligned}\left\|\mathbf{x}_j^0 - \mathbf{x}_i^0\right\|_2^2 &= \left(\mathbf{x}_j^0 - \mathbf{x}_i^0\right)^2 \\ &= \left\|R_i\left(\mathbf{x}_j^0 - \mathbf{x}_i^0\right)\right\|_2 + \left\|R_j\left(\mathbf{x}_j^0 - \mathbf{x}_i^0\right)\right\|_2 = (R_i + R_j)\left\|\mathbf{x}_j^0 - \mathbf{x}_i^0\right\|_2 \quad ,\end{aligned}$$

and thus,

$$\left\|\mathbf{x}_j^0 - \mathbf{x}_i^0\right\|_2 = R_i + R_j \quad ,$$

i.e., the distance between the centers of the ellipsoids is the sum of the radii as in (2.4). In general, the left-hand side of (2.36), is the distance of the centers of both centers projected onto $\mathbf{n}_{ij}^{\mathrm{H}}$, while the right-hand side is the sum of the distances from each center to the point where each ellipsoid touches the hyperplane.

We can also use the half-space approach to fit the ellipsoids into the box. For $d = 1$ we have

$$d_1^{\mathrm{R}} = 0 \leq \mathbf{n}_1^{\mathrm{R}}\mathbf{x}^0 - \left\|\mathsf{L}\mathbf{n}_1^{\mathrm{R}}\right\|_2 \quad , \mathbf{n}_1^{\mathrm{R}} := (+1, 0, 0) \tag{2.38}$$

for placing the ellipsoid to the right of the left plane or wall, *resp.*, of the box, and

$$d_1^{\mathrm{L}} = x_1^{\mathrm{R}} \geq -\mathbf{n}_1^{\mathrm{L}}\mathbf{x}^0 + \left\|\mathsf{L}\mathbf{n}_1^{\mathrm{L}}\right\|_2 \quad , \mathbf{n}_1^{\mathrm{L}} := (-1, 0, 0) \quad . \tag{2.39}$$

for placing the ellipsoid to the left of the right plane of the box. Similarly, for $d = 2$ and $d = 3$ we derive

$$d_2^{\mathrm{R}} = 0 \leq \mathbf{n}_2^{\mathrm{R}}\mathbf{x}^0 - \left\|\mathsf{L}\mathbf{n}_2^{\mathrm{R}}\right\|_2 \quad , \mathbf{n}_2^{\mathrm{R}} := (0, +1, 0) \tag{2.40}$$

$$d_2^{\mathrm{L}} = x_2^{\mathrm{R}} \geq -\mathbf{n}_2^{\mathrm{L}}\mathbf{x}^0 + \left\|\mathsf{L}\mathbf{n}_2^{\mathrm{L}}\right\|_2 \quad , \mathbf{n}_2^{\mathrm{L}} := (0, -1, 0) \quad , \tag{2.41}$$

and, for the upper side of the rectangular box, as displayed in Fig. 4, we obtain

$$d_3^{\mathrm{R}} = 0 \leq \mathbf{n}_3^{\mathrm{R}}\mathbf{x}^0 - \left\|\mathsf{L}\mathbf{n}_3^{\mathrm{R}}\right\|_2 \quad , \mathbf{n}_3^{\mathrm{R}} := (0, 0, +1) \tag{2.42}$$

$$d_3^{\mathrm{L}} = x_3^{\mathrm{R}} \geq -\mathbf{n}_3^{\mathrm{L}}\mathbf{x}^0 + \left\|\mathsf{L}\mathbf{n}_3^{\mathrm{L}}\right\|_2 \quad , \mathbf{n}_3^{\mathrm{L}} := (0, 0, -1) \quad . \tag{2.43}$$

If we use the half-space approach for both, separating ellipsoids and fitting ellipsoids into the box, we do not resort to matrix A at all, except for plotting the ellipsoids. This results in significantly fewer variables and constraints.

2.4 Comments on the structure of the problem

Before we enhance the model formulation by symmetry breaking constraints (Sect. 2.5), let us summarize the models and make some structural comments: All model consists of the trilinear objective function (2.1) and the linear constraints (2.25). Depending on which formulation we select to represent R

1. R1: [(2.12) and (2.13)],
2. R2: [(2.9), (2.8), and the bounds $-1 \leq v_d \leq +1$ and $-1 \leq w_d \leq +1$],
3. R3: [(2.14) and (2.15)],

and which formulation we select to separate ellipsoids and ensure non-overlap,

1. S1: separating hyperplanes using the KKT conditions with bilinear terms only [(2.11) and (2.16), (2.19)-(2.24), (2.30), (2.31)],

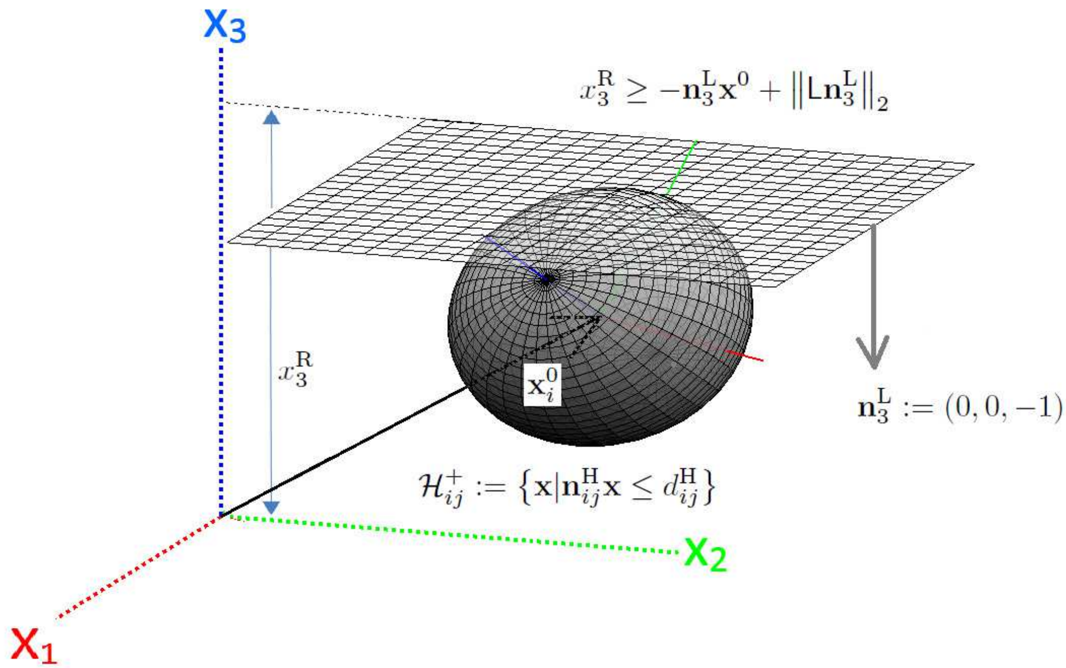

Fig. 4 Ellipsoid placed under the upper side, or plane, respectively, of the rectangular box for $d = 3$ and $\mathbf{n}_3^{\mathrm{L}} := (0, 0, -1)$. This illustrates formula (2.43).

2. S2: separating hyperplanes using the KKT conditions with bilinear and quadrilinear terms [(2.11) and (2.16), (2.19)-(2.24), (2.30), (2.31)], or
3. S3: the half-space approach [(2.34), (2.35), and (2.38)-(2.43)]

the model involves bilinear, a few trilinear or a significant number of quadrilinear terms caused by (2.33). Cafieri et al. (2009, [1]) show how to deal with quadrilinear terms. Alternatively, we could just use the trilinear terms caused by (B.74), 1 equation with 27 trilinear terms for each i, and (2.29), 3 equations with 3 trilinear terms for each ellipsoid and separation plane.

Considering all combinations of R1 to R3, and S1 to S3, we obtain a total of 9 different formulations for the ellipsoid packing problem are derived. In Subsection 2.7 we summarize the concise and best model formulation, EPP, which is basically the combination R1 and S3. Only in a very few cases, R2 coupled with S1 is superior to EPP. From the underlying structure, one might expect that S1 and S2 should have a positive effect on improving the lower bounds. Unfortunately, this is only the case for a few special cases with two ellipsoids.

The EPP is suitable to be solved by general purpose algorithms and software packages, but it is not obvious, which formulation is more suitable to a global solver at hand.

2.5 Symmetry breaking

Already in the 2D case of cutting ellipses, see Sect. 2.3 in KR14, symmetry was discussed as a problem. In the 3D case of ellipsoid, symmetry is even more a problem due to the third semimajor axis of ellipsoids. Additionally, the box has a third dimension and, therefore, more planes of symmetry at which we can reflect the solution. Although, we cannot completely reduces all symmetries, it is worthwhile to break at least a few.

A first symmetry to break is the size of the rectangular box. We enforce that length is greater or equal width, and width is greater or equal height, *i.e.*,

$$x_1^{\mathrm{R}} \leq x_2^{\mathrm{R}} \quad , \quad x_2^{\mathrm{R}} \leq x_3^{\mathrm{R}} \quad . \tag{2.44}$$

Given any feasible ellipsoid configuration in an rectangular box, we can construct alternative configurations fitting into the same box by reflections at axes in the box in the three coordinate axes. We destroy this symmetry partly, by enforcing that the center of *one* of the ellipsoids, for instance, the one with the largest volume, is positioned in the first octant of the box. If ι is the index of that ellipsoid. Then, the inequalities $x_{\iota d}^0 \leq \frac{1}{2} x_d^{\mathrm{R}}$ for all d break this symmetry. Unfortunately, many symmetries remain for the other ellipsoids.

If identical ellipsoids should be packed, we destroy the resulting symmetry by sorting them from left to right. We collect all pairs (i,j) of identical ellipsoids in the set $\mathcal{I}^{\mathrm{co}}$ (we assume ordered pairs $i<j$) and apply the ordering inequalities

$$x_{i1}^0 \leq x_{j1}^0 \quad , \quad \forall (i,j) \in \mathcal{I}^{\mathrm{co}} \quad . \tag{2.45}$$

While so far, we have only considered the symmetry regarding the center of the ellipsoids, there is, unfortunately, rotational symmetry. We consider rotation angles in the interval $[0°, 180°]$. Independent on whether we use the Eulerian angles, or one axis and one angle to represent rotated ellipsoids, we are facing the problem that a rotation of 180° degrees reproduces the original unrotated ellipsoid in shape – and thus the same size of the box.

2.6 Deriving lower and upper bounds via sphere packings and inner boxes.

To derive a lower and upper bound on the minimal volume of the box by V^- (V^+) via sphere packings, we proceed as in the 2D case for ellipses (Sect. 2.5 in KR14) and denote the lower and upper bound obtained by the inner sphere (outer sphere) packing by $V^{\mathrm{ci},-}$ and $V^{\mathrm{ci},+}$.

We can now tighten the bounds on the length, L, width, W, and height, H, of the box by solving the inner and outer sphere problems. It is $L \cdot W \cdot H \leq V^{\mathrm{ci},+}$ and $LW \leq V^{\mathrm{ci},+}/H \leq V^{\mathrm{ci},+}/S_3^-$. The minimum width, S_3^-, of the box, could be the maximum of all axis c_i, providing an upper bound on the product of length and height. Similarly, by using $V^{\mathrm{ci},-}$, we get a lower bound on LW.

For a given volume v, we can derive a corresponding upper bound of the height of the ellipsoid. This follows from the symmetry breaking constraint (2.44) and results in

$$x_3^{\mathrm{R}} \leq \sqrt[3]{v} \quad . \tag{2.46}$$

Inner rectangular boxes can be computed by maximizing the volume of that box subject to contained in the ellipsoid. In Appendix B.3 we show that box has only half the volume of the ellipsoid. Thus, for ellipsoids with $a \gg b > c$ it might be better to work with an outer box of size $(2a, 2b, 2c)$. This will not give a lower bound but a denser packing, if we find a way to pack such small boxes.

2.7 The complete and concise model formulation

Based on numerical test runs during the test phase, many of them summarized in Section 3, we obtain the following complete and concise model formulation EPP, which, in its core, is based on the constraints blocks R1 and S3 described in Subsection 2.4.

The *minimum volume*, trilinear objective function

$$z = v = x_1^{\mathrm{R}} x_2^{\mathrm{R}} x_3^{\mathrm{R}} \quad . \tag{2.47}$$

The *determinant condition*

$$\begin{aligned} 1 = \det \mathsf{R} = & R_{11}R_{22}R_{33} - R_{11}R_{23}R_{32} - R_{12}R_{21}R_{33} \\ & + R_{12}R_{31}R_{23} + R_{21}R_{13}R_{32} - R_{13}R_{22}R_{31} \quad . \end{aligned} \tag{2.48}$$

on the free rotation matrix R involving 6 trilinear terms for each ellipsoid i.

The *orthonormality conditions* established by six scalar products of row m ($\mathbf{r}_m$) and column n ($\mathbf{r}_n$) of R

$$\mathbf{r}_m^\top \mathbf{r}_n = \delta_{mn} \quad , \quad \forall \{mn|m \geq n\} \quad ; \tag{2.49}$$

again, for each ellipsoid i.

Fit the ellipsoids into the rectangular box (upper limit)

$$x_{id}^0 \geq c_i \quad , \quad \forall \{id\} \qquad \text{and} \qquad x_{id}^0 + c_i \leq x_d^{\mathrm{R}} \quad , \quad \forall \{id\} \quad . \tag{2.50}$$

Fit the ellipsoids into the box. For $d = 1$ we have for each ellipsoid

$$d_1^{\mathrm{R}} = 0 \leq \mathbf{n}_1^{\mathrm{R}} \mathbf{x}^0 - \left\| \mathsf{L} \mathbf{n}_1^{\mathrm{R}} \right\|_2 \quad , \mathbf{n}_1^{\mathrm{R}} := (+1, 0, 0) \tag{2.51}$$

for placing the ellipsoid to the right of the left plane or wall, *resp.*, of the box, and

$$d_1^{\mathrm{L}} = x_1^{\mathrm{R}} \geq -\mathbf{n}_1^{\mathrm{L}} \mathbf{x}^0 + \left\| \mathsf{L} \mathbf{n}_1^{\mathrm{L}} \right\|_2 \quad , \mathbf{n}_1^{\mathrm{L}} := (-1, 0, 0) \quad . \tag{2.52}$$

for placing the ellipsoid to the left of the right plane of the box. Similarly, for $d = 2$ and $d = 3$ we derive for each ellipsoid

$$d_2^{\mathrm{R}} = 0 \leq \mathbf{n}_2^{\mathrm{R}} \mathbf{x}^0 - \left\| \mathsf{L} \mathbf{n}_2^{\mathrm{R}} \right\|_2 \quad , \mathbf{n}_2^{\mathrm{R}} := (0, +1, 0) \tag{2.53}$$

$$d_2^{\mathrm{L}} = x_2^{\mathrm{R}} \geq -\mathbf{n}_2^{\mathrm{L}} \mathbf{x}^0 + \left\| \mathsf{L} \mathbf{n}_2^{\mathrm{L}} \right\|_2 \quad , \mathbf{n}_2^{\mathrm{L}} := (0, -1, 0) \quad , \tag{2.54}$$

and

$$d_3^{\mathrm{R}} = 0 \leq \mathbf{n}_3^{\mathrm{R}} \mathbf{x}^0 - \left\| \mathsf{L} \mathbf{n}_3^{\mathrm{R}} \right\|_2 \quad , \mathbf{n}_3^{\mathrm{R}} := (0, 0, +1) \tag{2.55}$$

$$d_3^{\mathrm{L}} = x_3^{\mathrm{R}} \geq -\mathbf{n}_3^{\mathrm{L}} \mathbf{x}^0 + \left\| \mathsf{L} \mathbf{n}_3^{\mathrm{L}} \right\|_2 \quad , \mathbf{n}_3^{\mathrm{L}} := (0, 0, -1) \quad . \tag{2.56}$$

The *difference of the centers* of ellipsoid i and j in axis direction d

$$d_{ijd}^{\mathrm{c}} = x_{id}^0 - x_{jd}^0 \quad , \quad \forall \{ijd|i > j\} \quad . \tag{2.57}$$

Affine transformation of the unit sphere

$$\mathsf{L} = \mathsf{R}\mathsf{\Lambda} \quad , \quad \mathsf{\Lambda} := \operatorname{diag}(a, b, c) \quad , \quad L_{imn} = R_{imn} \Lambda_{inn} \quad , \quad \forall \{imn\} \quad . \tag{2.58}$$

Non-overlap of ellipsoids is ensured by

$$\mathbf{n}_{ij}^{\mathrm{H}} \left(\mathbf{x}_j^0 - \mathbf{x}_i^0 \right) \geq \left\| \mathsf{L}_i \mathbf{n}_{ij}^{\mathrm{H}} \right\|_2 + \left\| \mathsf{L}_j \mathbf{n}_{ij}^{\mathrm{H}} \right\|_2 \quad ,$$

which in components reads

$$\sum_d n^{\rm H}_{ijd} d^{\rm c}_{ijd} \geq \sqrt{\sum_d \sum_m \left(L_{imd} n^{\rm H}_{ijm} \right)^2} + \sqrt{\sum_d \sum_m \left(L_{jmd} n^{\rm H}_{ijm} \right)^2} \quad , \quad \forall \{ij | i > j\} \quad . \tag{2.59}$$

The *upper limit on the smallest dimension* of the rectangular box

$$x^{\rm R}_3 \leq \sqrt[3]{v} \quad . \tag{2.60}$$

A necessary condition for ellipsoid i and j not to overlap and *useful cut* improving the lower bound on volume is the inner sphere approximation exploiting the smallest semi-axes

$$\left| \mathbf{x}^0_i - \mathbf{x}^0_j \right|^2_2 := \sum\nolimits_{d=1}^{3} \left(x^0_{id} - x^0_{jd} \right)^2 \geq (c_i + c_j)^2 \quad , \quad \forall \{ij | i < j\} \quad . \tag{2.61}$$

Normalization of the normal vector $\mathbf{n}^{\rm H}_{ij}$ to a unit vector, *i.e.*,

$$\left\| \mathbf{n}^{\rm H}_{ij} \right\|_2 = 1 \quad \Leftrightarrow \quad \sum_d \left(n^{\rm H}_{ijd} \right)^2 = 1 \quad , \quad \forall \{ij | i < j\} \quad . \tag{2.62}$$

Symmetry breaking: The length of the box is greater or equal width, and width is greater or equal height, *i.e.*,

$$x^{\rm R}_1 \leq x^{\rm R}_2 \quad , \quad x^{\rm R}_2 \leq x^{\rm R}_3 \quad . \tag{2.63}$$

A selected ellipsoid ι is located in the first octant of the rectangular box

$$x^0_{\iota d} \leq \frac{1}{2} x^{\rm R}_d \quad , \quad \forall d \quad . \tag{2.64}$$

Table 2 shows the number of variables and constraints according to each equation.

Table 2 Summary of all related equations, Number, $N_{\rm var}$, of variables and number, $N_{\rm con}$, constraints

Equations	**variables**	$N_{\rm var}$	$N_{\rm con}$
1) objective function z=v, (2.47)	$v, x^{\rm R}_1, x^{\rm R}_2, x^{\rm R}_3$	1+3	-
2) det R = 1 , (2.48)	R_{ij}	$9 \times n$	$1 \times n$
3) orthonormality conditions, (2.49)	(R_{ij})	-	$6 \times n$
4) rectangular box upper limit, (2.50)	x^0_{id}	$3 \times n$	$2 \times 3 \times n$
5) planes of the box, (2.51) to (2.56)	(x^0_{id}, L_{imn})	-	$6 \times n$
6) difference of the centers of ellipsoid, (2.57)	$(d^{\rm C}_{ijd}, x^0_{id})$	$3 \times m$	$3 \times m$
7) Affine transformation, (2.58)	$L_{imn}, (R_{ij})$	$3 \times 3 \times n$	$3 \times 3 \times n$
8) Non-overlap of ellipsoids , (2.59)	$n^{\rm H}_{ijd}, (L_{imn}, d^{\rm C}_{ijd})$	$3 \times m$	m
9) upper limit on $x^{\rm R}_3$, (2.60)	(v, $x^{\rm R}_3$)	-	1
10) condition for ellipsoid i and j not to overlap, (2.61)	(x^0_{id})	-	m
11) Normalization of $n^{\rm H}_{ij}$, (2.62)	$(n^{\rm H}_{ijd})$	-	m
12) Symmetry breaking, (2.63)	$(x^{\rm R}_1, x^{\rm R}_2, x^{\rm R}_3)$	-	2
13) ellipsoid in the first octant of the box, (2.64)	$(x^{\rm R}_1, x^{\rm R}_2, x^{\rm R}_3, x^0_{id})$	-	3

This model, for n ellipsoids, $D = 3$ and $m = n(n-1)/2$ has a total of

$$1 + 3 + 9n + 3n + 3m + 9n + 3m = 4 + 21n + 6m \tag{2.65}$$

variables and

$$1n + 6n + 2 \times 3n + 6n + 3m + 9n + m + 1 + m + m + 2 + 3 = 6 + 28n + 6m \tag{2.66}$$

constraints.

3 Numerical experiments

Using some of the global solvers available in `GAMS`, *i.e.*, Antigone [15], Baron [18], and LindoGlobal [12], and the model formulation EPP summarized in Subsection 2.7, we perform the following numerical experiments:

1. Packing one ellipsoid – gap closed, *i.e.*, $|z^{\mathrm{ub}} - z^{\mathrm{lb}}| \leq 10^{-4}$
2. Treating Spheres as ellipsoids (2 & 3 ellipsoids) – gap closed
3. One ellipsoid plus one ellipsoid close to a sphere – gap closed for some experiments
4. Monolithic experiments with 2 to 50 ellipsoids.
5. Monolithic experiments with 6 to 50 congruent ellipsoids
6. Polylithic experiments with seven to 7 to 50 arbitrary ellipsoids.

All test cases used for the computations are listed in Table 3. We used the following computers for the numerical experiments.

Platform 1: Dual core machine with CPUs @ 2.5 GHz (Intel booth technology) 48GB RAM and 250 GB HDD running Windows 7.

Platform 2: Dual-six core machine with CPUs @ 3.3 GHz, 48GB RAM and 1TB HDD running Win2008 Server.

All computations utilize only a single core of the machines specified above.

3.1 Proof-of-Concept: Treating spheres as ellipsoids

We use the ellipsoid packing formulation (EPP) to show the correctness of the approach by solving two sphere packing instances, S1 and S2, with two and three spheres and radii R_i specified in Table 4:

The spherical problem is solved with a relative gap smaller than 10^{-8} in 2 seconds using one of the solvers above.

In the first two columns of Table 5, we refer to the problem instance; v^* is the globally minimal volume of the box as calculated via a sphere packing formulation, *cf.* Sect. 2.1.1. In the other columns, we display the lower bound, V^-, the upper bound, V^+, on the minimal volume of the rectangular box, and the computational time for (EPP) with three global solvers embedded in `GAMS`. We observe that (1) the results computed with EPP are consistent with the global optima computed with the sphere packing formulation, (2) global optimality can only be proven for S1 within the time limit, and (2) the global solvers perform very differently in terms of lower bounds and the quality of computed feasible solutions.

3.2 Monolith

Table 6 summarizes the computational results for the monolith formulation (EPP). Unfortunately, all three current state-of-the-art global solvers have difficulties closing the gap for the tested instances.

Table 3 Ellipsoid packing instances with the semi-axes of the ellipsoids and lower and upper bounds on the size of the rectangular box. The last column gives the sum of all ellipsoid volumes $V = \sum_i V_i$.

test case	(a_i, b_i, c_i)	S_d^-	S_d^+	V
Ellipsoid packing instances "regular":				
TC01a	$(3, 2, 1)$	(0,0,0)	(10,10,10)	25.13274
TC01b	"TC01a"	(0,0,0)	(6,4,2)	25.13274
TC02a	$(2, 1.5, 1)$, $(1.5, 1, 0.7)$	(0,0,0)	(6,3.1,2)	16.96460
TC02b	"TC02a"	(0,0,0)	(10,4,4)	16.96460
TC02c	$(2, 1.9, 1.8)$, $(1, 0.95, 0.9)$	(4.5,2.5,1.5)	(6,4,4)	32.23274
TC02d	$(2, 1.95, 1.9)$, $(1, 0.98, 0.95)$	(4.5,2.5,1.5)	(6,4,4)	34.93870
TC02e	$(2, 2, 2)$, $(1, 0.55, 0.40)$	(4,4,4)	(4.15,4,4)	34.43186
TC02f	$(2, 2, 2)$, $(2, 1.98, 1.95)$	(4,4,4)	(8,4,4)	65.85616
TC02g	$(2, 2, 2)$, $(2, 1.94, 1.90)$	(4,4,4)	(10,10,10)	64.39008
TC03a	"TC02b" + $(1, 0.8, 0.6)$	(0,0,0)	(5,4,4)	18.97522
TC03c	"TC03a"	(0,0,0)	(20,10,10)	18.97522
TC04a	"TC03a" + $(0.9, 0.7, 0.5)$	(0,0,0)	(99,99,99)	20.29469
TC04b	"TC04b"	(0,0,0)	(6,6,6)	20.29469
TC05a	"TC03a" + $(0.9, 0.75, 0.5)$ + $(0.8, 0.6, 0.3)$	(0,0,0)	(20,20,20)	20.99212
TC07a	"TC05a" + $(1.2, 0.9, 0.4)$, $(1.1, 0.9, 0.4)$	(0,0,0)	(99,99,99)	24.46044
TC08a	"TC07a" + $(1.8, 1.4, 1.2)$	(0,0,0)	(99,99,99)	37.12734
TC09a	$(2, 1.5, 1.0)$, $(1.8, 1.4, 1.2)$, $(1.5, 1.0, 0.8)$, $(1.2, 0.9, 0.7)$, $(1.1, 0.9, 0.4)$, $(1.0, 0.8, 0.4)$, $(0.9, 0.75, 0.50)$, $(0.8, 0.6, 0.3)$, $(0.7, 0.4, 0.2)$	(0,0,0)	(99,99,99)	37.36191
TC10a	$(2, 1.5, 1.0)$, $(1.5, 1.0, 0.7)$, $(1.0, 0.8, 0.6)$, $(0.9, 0.75, 0.7)$, $(0.8, 0.6, 0.4)$, $(1.2, 0.9, 0.4)$, $(1.1, 0.9, 0.4)$, $(1.8, 1.4, 1.2)$, $(0.7, 0.4, 0.2)$ $(1.3, 1.2, 0.9)$	(0,0,0)	(7,6,4)	43.24298
Identical ellipsoids; total volume of these n identical ellipsoids is $\frac{4}{3}\pi abcn \approx 5n/3$:				
TS06s01	$6 \times (1, 0.8, 0.5)$	(0,0,0)	(5,2.5,2)	10.05310
TS06s03	$6 \times (1, 0.8, 0.5)$	(0,0,0)	(99,99,99)	10.05310
TS08	$8 \times (1, 0.8, 0.5)$	(0,0,0)	(999,999,999)	13.40413
TS09	$9 \times (1, 0.8, 0.5)$	(0,0,0)	(999,999,999)	15.07964
TS10	$10 \times (1, 0.8, 0.5)$	(0,0,0)	(999,999,999)	16.75516
TS11	$11 \times (1, 0.8, 0.5)$	(0,0,0)	(999,999,999)	18.43068
TS12	$12 \times (1, 0.8, 0.5)$	(0,0,0)	(999,999,999)	20.10619
TS13	$13 \times (1, 0.8, 0.5)$	(0,0,0)	(999,999,999)	21.78171
TS14	$14 \times (1, 0.8, 0.5)$	(0,0,0)	(999,999,999)	23.45723
TS15	$15 \times (1, 0.8, 0.5)$	(0,0,0)	(999,999,999)	25.13274
TS16	$16 \times (1, 0.8, 0.5)$	(0,0,0)	(999,999,999)	26.80826
TS17	$17 \times (1, 0.8, 0.5)$	(0,0,0)	(999,999,999)	28.48377
TS18	$18 \times (1, 0.8, 0.5)$	(0,0,0)	(999,999,999)	30.15929
TS19	$19 \times (1, 0.8, 0.5)$	(0,0,0)	(999,999,999)	31.83481
TS20	$20 \times (1, 0.8, 0.5)$	(0,0,0)	(999,999,999)	33.51032
TS30	$30 \times (1, 0.8, 0.5)$	(0,0,0)	(999,999,999)	50.26548
TS50	$30 \times (1, 0.8, 0.5)$	(0,0,0)	(999,999,999)	83.77580
TS60	$60 \times (1, 0.8, 0.5)$	(0,0,0)	(120,120,120)	100.53096
TS70	$70 \times (1, 0.8, 0.5)$	(0,0,0)	(140,140,140)	117.28613
TS80	$80 \times (1, 0.8, 0.5)$	(0,0,0)	(160,160,160)	134.04129
TS90	$90 \times (1, 0.8, 0.5)$	(0,0,0)	(180,180,180)	167.55161
TS100	$100 \times (1, 0.8, 0.5)$	(0,0,0)	(200,200,200)	167.55161
TS100b	$100 \times (1, 0.8, 0.5)$	(0,0,0)	(10,10,10)	167.55161

Table 4 Setup of the numerical experiment treating spheres as ellipsoids.

	R_1	R_2	R_3	v	x_1^{R}	x_2^{R}	x_3^{R}
S1	1	1		16	4	2	2
S2	2	1.5	1	118.675265	6.9278	4.2826	4

Table 5 Packing spheres as ellipsoids with fixed rotation angles $\theta_i \equiv 0$, or $R = \text{diag}(1, 1, 1)$, respectively. Test cases are S1 and S2 defined in Table 4. Problem S1 was solved instantaneously by all solver, *i.e.*, in less than a second. For problem S2, the CPU time limit of 12,000 seconds was reached. GAMS 24.4 with platform 1.

test case	v^*	**Antigone** V^-	V^+	**Baron** V^-	V^+	**LindoGlobal** V^-	V^+
S1	16.00000	15.9900	16.0000	15.9900	16.0000	16.0031	16.0126
S2	118.675265	112.1000	118.6753	110.8071	118.6753	83.3175	120.9696

Table 6 Monolith: Packing ellipsoids with (EPP) using the half-space approach. CPU time limit was 4 hours for experiments TC02a to TC02f, and 15, 30, or 45 minutes, resp., for all others; `GAMS` 24.4; platform 1. Experiments TC02a to TC02f were performed with the restriction of the Eulerian angles to the interval [0,90] degrees. With this restriction the lower bound increased steadily, while the best upper bound obtained is identical to that one resulting from Eulerian angles restricted to [0,90]. Note, how slowly the lower bound increases when we allow 48 hours to solve TC02a. Case TC10a is displayed in Fig. 5.

test case	**Antigone** V^-	V^+	**mm:ss**	**Baron** V^-	V^+	**m:ss**	**LindoGlobal** V^-	V^+	**m:ss**
TC02a	V	32.40000	30:00	29.85799	32.40000	4h	27.71865	32.40000	10:00
TC02a	.	.	.	30.84000	32.40000	48h	.	.	.
TC02b	22.50000	32.40000	30:00	30.75311	32.40000	4h	27.41398	32.40000	10:00
TC02c	58.32000	75.33625	30:00	70.07250	75.33625	4h	61.56000	75.33625	10:00
TC02d	64.98000	82.68374	30:00	76.93540	82.68374	4h	70.25929	82.68374	10:00
TC02e	64.00000	67.67309	30:00	64.00000	67.67309	4h	64.00000	67.67309	10:00
TC02f	72.00000	126.39920	30:00	117.75470	126.39920	4h	119.90176	126.39920	10:00
TC02g	72.00000	124.79276	30:00	111.03900	124.79276	4h	118.64514	124.79276	10:00
TC03a	V	35.64096†	03:20	V	35.64096†	02:35	V	37.50108	04:30
TC03b	V	35.64096†	03:20	V	35.64096†	02:35	V	37.50108	04:30
TC04a	V	–	30:00	V	38.90865	07:59	V	39.60000	10:49
TC04b	V	–	30:00	V	39.66012	00:02	V	39.66012	00:37
TC05a	V	–	30:00	V	39.50374	00:05	V	39.67963	13:23
TC07a	V	–	30:00	V	46.25267	00:09	V	50.67277	13:28
TC08a	V	–	30:00	V	71.01258	00:19	V	**70.90260**	14:08
TC09a	V	–	30:00	V	75.22376	00:15	V	78.96324	21:45
TC10a	V	–	30:00	V	83.63259	02:26	V	84.79978	11:48
TS11	V	–	30:00	V	34.14894	06:53	V	37.08669	17:38
TS12	V	–	30:00	V	38.40137	00:27	V	–	30:00
TS13	V	–	30:00	V	41.53936	01:08	V	43.94060	08:34
TS14	V	–	30:00	V	43.72803	01:16	V	48.78287	10:07
TS15	V	–	30:00	V	51.00793	01:31	V	–	30:00
TS16	V	–	30:00	V	53.85946	06:33	V	–	30:00
TS17	V	–	30:00	V	53.76414	01:41	V	55.61720	02:03
TS18	V	–	30:00	V	58.91550	01:41	V	**57.57058**	30:00
TS19	V	–	30:00	V	60.52080	14:25	V	2052.743616	30:01
TS20	V	–	30:00	V	62.12678	01:57	V	111.09076	30:02
TS30	V	–	30:00	V	103.40513	16:40	V	177.68667	30:04
TS50	V	–	30:00	V	215.00144	30:02	V	–	30:04
TS60	V	–	30:00	V	215.00144	30:02	V	–	30:04
TS70	V	–	180:00	V	340.65796	116:32	V	–	180:00
TS80	V	–	180:00	V	446.71011	136:53	V	–	180:00
TS90	V	–	360:00	V	–	360:00	V	–	360:00
TS100	V	–	360:00	V	–	360:00	V	–	360:00
TS100b	V	–	1440:00	V	477.29091	732:21	V	–	1440:00
†	obtained when using the KKT approach with bilinear terms only								
–	no feasible solution found								

Separating hyperplanes exploiting the half-space approach lead to problems with the fewest numbers of variables. Sometimes, however, we obtain better solutions when we use the somewhat more complicated approach using the KKT conditions with bilinear terms only.

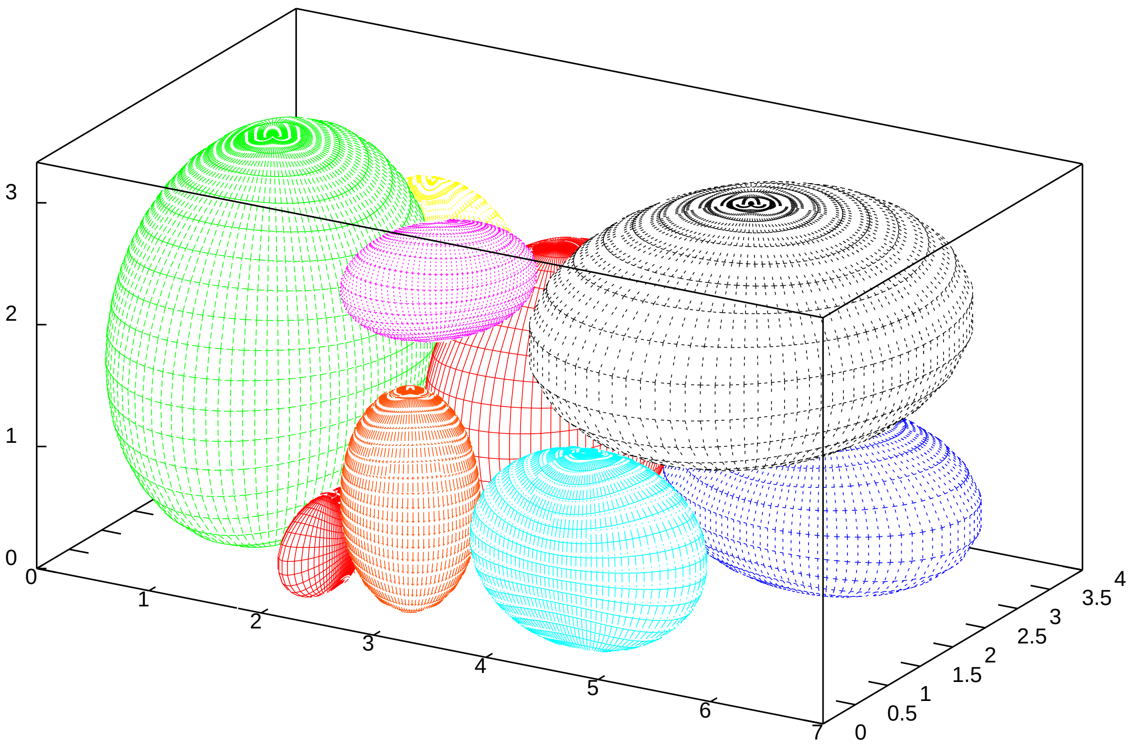

Fig. 5 Packing 10 ellipsoids –case TC10a– using the monolithic version of the EPP.

3.2.1 Inner and outer spheres

Table 7 displays the lower bounds based on the volumes of the ellipsoids ($\sum_i V_i$), the lower bounds, $V^{\mathrm{ci},-}$, resulting from the inner sphere problem, and an upper bound, $V^{\mathrm{ci},+}$, derived from the outer sphere problem. The lower bounds obtained from the inner sphere packings are significantly better than the sum of all volumes of the ellipsoids when the majority of the ellipsoids has aspect ratio close to 1; otherwise, the sum of all volumes of the ellipsoids exceeds $V^{\mathrm{ci},-}$. As the initial lower bounds obtained by the solvers for the EPP are significantly smaller, we use $\max\{\sum_i V_i, V^{\mathrm{ci},-}\}$ as the lower bound for the EPP. The upper bounds obtained by the outer-spheres are, unfortunately, usually only very weak bounds.

3.2.2 Identical ellipsoids

Identical ellipsoid packing problems are easier to solve than the general EPP as we can apply the symmetry breaking inequalities (2.45), or the simpler inequality $x_i \leq x_j$ for $i < j$. Similar as in the 2D case for ellipses, we can also construct analytic, symmetric ellipsoid configurations. This allows us to double-check our models, benchmark the solvers and compare the solution to unsymmetrical configurations.

Table 6 contains computations for identical ellipsoids using the monolith formulation (EPP). With only 15 minutes of CPU time, the lower bounds do not increases above the sum of the volume of all ellipsoids. This behavior does not change when allowing 30 or 60 minutes, or even 12 hours.

Table 7 Comparing volume of ellipsoids, inner spheres, outer spheres and best monolithic and polylithic solution found (taken from Table 6 or Table 8). For TC02a to TC04b the relative gap, after 30 minutes or less, for solving the inner and outer spheres problem was less than 10^{-8}, for TC05a 2×10^{-5}. For TC07a and higher we have, after 30 minutes, relative gaps of 30, 40, and up to 90 %, *i.e.*, the solution of the outer sphere problem is only of limited use. In addition to the time efficiency of the polylithic approach, in various cases displayed in bold face, it produces better solutions as the monolith.

test case	$\sum_i V_i$	$V^{\mathrm{ci},-}$	$V^{\mathrm{ci},+}$	V^{m}	V^{p}
TC02a	16.96460	13.38482	110.84521	32.40000	32.40000
TC02b	16.96460	22.50000	110.84523	32.40000	32.40000
TC02c	32.23274	65.85202	90.33199	75.33625	75.33625
TC02d	34.93870	77.44839	90.33202	82.68374	82.68374
TC02e	34.43186	64.00000	90.33200	67.67309	67.67309
TC02f	65.85616	126.38987	128.00000	126.39920	126.39959
TC02g	64.39008	124.75896	128.00000	124.79276	124.79276
TC03a	18.97522	15.41652	118.67534	35.64096	37.31679
TC03b	18.97522	15.41652	118.67534	35.64096	37.31679
TC04a	20.29469	15.97308	120.59568	38.55590	38.55589
TC04b	20.29469	15.97309	120.59568	39.66012	39.66012
TC05a	20.99212	15.97304	120.59560	39.50374	**39.28794**
TC07a	24.46044	16.04026	145.99118	46.25267	**45.43634**
TC08a	37.12734	30.79035	194.95129	70.90260	**70.24573**
TC09a	38.67719	34.45173	199.49578	74.24859	74.39517
TC10a	43.24298	36.70484	218.59640	84.79978	**80.67366**
TS11	18.43068	10.92820	87.42563	34.14894	**34.00782**
TS12	20.10619	12.00000	96.00000	38.40137	**36.19232**
TS13	21.78171	13.06218	104.49742	41.53936	**39.93079**
TS14	23.45723	13.66025	109.28203	43.72803	**42.40982**
TS15	25.13274	14.92820	119.42563	51.00793	**47.51635**
TS16	26.80826	15.66923	128.00000	53.85946	**51.12193**
TS17	28.48377	17.19616	137.56922	53.76414	**52.56416**
TS18	30.15929	17.41025	139.28203	57.57058	**56.36222**
TS19	31.83481	18.66025	149.28203	60.52080	60.60758
TS20	33.51032	19.12436	152.99485	62.12678	64.46473
TS30	50.26548	28.03942	222.85125	103.40513	**94.63151**
TS50	83.77580	48.07488	391.93313	215.00144	**152.38815**
TS60	100.53096	—	—	218.17868	257.05663
—	no feasible point found within the time limit				

The larger the number of ellipsoids, the more "symmetrical" solutions we obtain, *i.e.*, the higher the degree of order in the packing, while for smaller number of ellipsoids the solutions are rather "asymmetrical" placements.

3.2.3 Summary of the monolithic experiments

Let us comment on the various approaches how we treat the separating hyperplanes and the rotation matrix $\mathbf{R}$. The half-space approach, S3, based on affine transformations of spheres has the smallest number of variables and constraints and works fastest. We can even find feasible points for 100 ellipsoids although that took about 12 hours using Baron. However, if we use the KKT-approach using only bilinear terms (S1), we can, in some instances, find better solutions. If we see an increase of the lower bound, then only with this approach. The KKT-approach using quadrilinear terms (S2) is not efficient.

The rotation matrix is best represented by R1 regarding the numerical performance. The many terms involved in R3 seem to be too complicated and increase the computing time. R2 is only superior when compared to R1 or R3, if we can restrict the angles to range [0,90] degrees as we did in a few experiments for two ellipsoids.

3.3 Polylithic

If the number of ellipsoids increases, the global solver have more and more difficulties to find a feasible point using the monolith. For the larger test instances (TS20, TS30, TS50, and TS60 to TS100b), only Baron can find a feasible points. Therefore, we have developed three polylithic approaches to compute feasible points:

1. P1: Unrotated ellipsoids i are placed at

$$x_{i1}^0 = a_i + 2a_i(i-1), \quad x_{i2}^0 = b_i, \quad x_{i3}^0 = c_i \quad .$$

   This approach works only, if the size of the box in x-direction is not smaller than $x_{n1}^0 = a_n$. With the normal vector $\mathbf{n}_{ij}^{\mathrm{H}} = (-1,0,0)$ of the separating hyperplane H_{ij} we get a feasible point easily. However, the global solver experience difficulties to improve on this starting point. Therefore, after some initial numerical experiments, we did not follow up on this approach.
2. P2: To begin with, we solve the outer-sphere approximation to all ellipsoids individually, from which we obtain the centers of the spheres and the size of the box. We place and fix the unrotated ellipsoids precisely at the centers computed. As we had an outer approximation, they fit into this box. Next, we compute separating hyperplanes consistent with this placements. Then, we relax all variables, and compute feasible points to the original problem. That way, we obtain feasible points up to 50 ellipsoids; see Table 8. This approach is expected to work the better the less the ellipsoids deviates from spheres. However, P2 is also limited by the size of the spheres problem which can be solved reasonably in time and quality.

Table 8 Polylithic: Packing ellipsoids using polylithic approach 2 based on outer spheres. CPU time limit was 15, 30, or 45 minutes, respectively; GAMS 24.4; platform 1. The problems have been solved with Baron and various time limits.

test case	Baron1 V^-	Baron1 V^+	Baron1 **mm:ss**	Baron2 V^-	Baron2 V^+	Baron2 **m:ss**	size of the box x_1^R	size of the box x_2^R	size of the box x_3^R
TC05a	V	39.92219	15:08	V	39.92219	15:08	6.654	3.000	2.000
TC07a	V	46.06638	25:05	V	46.00333	45:35	4.000	3.839	3.000
TC08a	V	71.43821	30:05	V	69.37830	50:19	4.412	4.412	3.670
TC09a	V	75.82589	30:05	V	75.50322	50:20	6.319	4.000	3.000
TC10a	V	88.03426	20:13	V	84.48749	50:34	6.824	3.872	3.332
TS08	V	24.24369	30:04	V	24.63693	65:48	3.487	3.476	2.000
TS09	V	28.34020	30:04	V	27.91272	65:38	3.764	3.764	2.000
TS10	V	30.67300	30:04	V	29.52895	65:04	3.916	3.916	2.000
TS11	V	35.99302	30:07	V	34.85208	65:07	4.483	4.015	2.000
TS12	V	36.19232	30:07	V	37.10278	65:06	7.116	2.543	2.000
TS13	V	39.93079	30:05	V	40.13174	65:05	4.828	4.135	2.000
TS14	V	42.40982	30:13	V	44.32968	65:05	5.796	3.658	2.000
TS15	V	47.51635	30:06	V	49.03190	65:07	4.874	4.874	2.000
TS16	V	51.12193	30:08	V	50.90590	65:05	4.309	3.970	2.988
TS17	V	53.55365	30:06	V	55.05772	65:07	4.982	3.796	2.832
TS18	V	57.28836	45:07	V	55.35534	95:14	4.563	3.562	3.525
TS19	V	60.60758	45:07	V	60.87294	95:10	4.553	4.393	3.030
TS20	V	64.46473	45:05	V	63.76019	95:07	4.799	4.504	2.982
TS30	V	94.63151	45:17	V	89.14050	95:12	7.369	6.421	2.000
TS50	V	152.38815	47:20	V	52.38815	96:30	34.861	4.371	1.000
TS60	V	–	–	V	192.90897	102:40	34.861	4.371	1.000
—	no feasible solution found within the time limit								

3. P3: This polylithic approach works similarly as H1 and H2 in KR14. Ellipsoids are filled into the box by a pre-given sequence along the positive x-axis. This approach, and the packing density ρ depends strongly on the sequence of ellipsoids selected to be placed. Therefore, it has its limits for large numbers of differently sized ellipsoids, while for identical ellipsoids it can work for very large numbers of ellipsoids.

We only report on the results of P2 as this approach can produce high quality solutions as long as we can solve the sphere packing problem reasonably, and because it is new while P3 has already been used earlier in the 2D cases of ellipse cutting. Although we find feasible packing solutions for up to 50, even 60 ellipsoids, we reach the limits of spheres problems which we can solve. The CPU limits in Tables 8 and 9 are only so large because we wanted to have a homogeneous set of computations. As the left part of Table 8 shows, it can be done in less time; actually, except for the larger cases with more than 30 ellipsoids, we find feasible points in 5 to 10 minutes. The need to resort to this polylithic approach is necessary when we use S1 to separate ellipsoids. If we use the half-space approach, S3, the monolithic approach can find feasible solution even for large problems although it may take many hours. In addition to the time efficiency of the polylithic approach, in various cases displayed in bold face in Table 7, it produces better solutions as the monolith.

Table 9 Polylithic: Packing ellipsoids using polylithic approach 2 based on outer spheres. CPU time limit was 15, 30, or 45 minutes, respectively; `GAMS` 24.4; platform 1. The problems have been solved with Antigone and Baron. The Baron results are the same as in Table 8.

test	**Antigone**			**Baron**			**size of the box**		
case	V^-	V^+	**mm:ss**	V^-	V^+	**m:ss**	x_1^R	x_2^R	x_3^R
TC05a	V	39.28794	15:45	V	39.92219	15:08	6.654	3.000	2.000
TC07a	V	45.43634	75:09	V	46.00333	45:35	4.000	3.839	3.000
TC08a	V	70.24573	80:11	V	69.37830	50:19	4.412	4.412	3.670
TC09a	V	74.39517	80:11	V	75.50322	50:20	6.319	4.000	3.000
TC10a	V	80.67366	80:17	V	84.48749	50:34	6.824	3.872	3.332
TS08	V	24.69427	95:16	V	24.63693	65:48	3.487	3.476	2.000
TS09	V	26.25337	95:16	V	27.91272	65:38	3.764	3.764	2.000
TS10	V	30.91687	95:17	V	29.52895	65:04	3.916	3.916	2.000
TS11	V	34.00782	95:17	V	34.85208	65:07	4.483	4.015	2.000
TS12	V	37.83346	95:12	V	37.10278	65:06	7.116	2.543	2.000
TS13	V	40.27221	95:10	V	40.13174	65:05	4.828	4.135	2.000
TS14	V	45.73893	95:14	V	44.32968	65:05	5.796	3.658	2.000
TS15	V	48.93781	95:14	V	49.03190	65:07	4.874	4.874	2.000
TS16	V	52.48874	95:14	V	50.90590	65:05	4.309	3.970	2.988
TS17	V	52.56416	95:14	V	55.05772	65:07	4.982	3.796	2.832
TS18	V	56.36222	125:22	V	55.35534	95:14	4.563	3.562	3.525
TS19	V	–	–	V	60.87294	95:10	4.553	4.393	3.030
TS20	V	–	–	V	63.76019	95:07	4.799	4.504	2.982
TS30	V	–	–	V	89.14050	95:12	7.369	6.421	2.000
TS50	V	–	–	V	52.38815	96:30	34.861	4.371	1.000
TS60	V	–	–	V	192.90897	102:40	34.861	4.371	1.000
—	no feasible solution found within the time limit								

4 Conclusions

We developed non-convex NLP approaches and models for packing ellipsoids into one rectangular box. Feasible ellipsoid packings can be solved with the current state-of-the art deterministic global solvers Antigone, Baron, LindoGlobal provided in `GAMS`. The more the ellipsoids deviate from spheres, the more difficult it is to improve the lower bound or to close the gap. As it is expected from the NP-hard nature of the ellipsoid packing problem, global solvers reach their limitations fast and it becomes a very challenging task for the solvers even to compute just a feasible point.

We obtain feasible points within minutes for small instances up to 20 objects. For the largest instance, 100 identical ellipsoids, we found a feasible solution after 12 hours. Alternatively, polylithic approaches allow us to obtain solution for up to 20 to 60. Solutions for more than 15-60 congruent ellipsoids can be obtained by P3, *i.e.*, sequential filling of boxes by adding 5 to 10 ellipsoids each time.

We experience that symmetry, degeneracy and to some extent also the bounds on the size of the rectangular box limit the size of the problems we are able to solve using this NLP approaches. Future work will target on packing 100 to 1000 ellipsoids using deterministic global solvers, improving the lower bounds and to tackle the ellipsoid design problem. In the design problem, the semi-axes would be unknown design variables. Using two or three different sets of congruent ellipsoids, we would improve the packing density.

Acknowledgements Thanks are directed to Prof. Dr. Siegfried Jetzke (Ostfalia Hochschule, Salzgitter, Germany) for his interest in this work, comments on the manuscript and discussion about the usefulness of ellipses and ellipsoids in real world problems. The author is grateful to Dr. Arash Rezaeian (WIEH Erdgashandelshaus, Berlin, Germany) for his careful proof reading and production of the figures.

A Notation

We begin with a summary of the notation used in the derivation of the model.

A	positive definite and symmetric matrix defining ellipsoids; we call this also the shape-rotation matrix.
$\mathbf{c}$	objective function coefficient vector of auxiliary problems; $\mathbf{c}^\top = (1,0,0)$ or $\mathbf{c}^\top = (0,1,0)$ or $\mathbf{c}^\top = (0,0,1)$
D_i	diagonal matrix for ellipsoid i with eigenvalues of A_i on the diagonal
δ_{mn}	Kronecker delta function takes value 1 if the indices m and n are equal, otherwise it takes the value zero 0
$\mathcal{L}(\mathbf{x},\bar{\lambda})$	Lagrangian function
λ_{id}	eigenvalue of matrix A_i; $\lambda_{i1} = a_i^{-2}$, $\lambda_{i2} = b_i^{-2}$, and $\lambda_{i3} = c_i^{-2}$
$\bar{\lambda}$	Lagrangian multiplier associated with ellipsoid equation
ρ	density of ellipsoids; $0 \le \rho \le 1$
$\mathsf{R}_{\theta i}$	rotation matrix for ellipsoid i at angle θ_i
x_{id}^-	minimal extension of ellipsoid i in dimension d
x_{id}^+	maximal extension of ellipsoid i in dimension d
ι	selected ellipsoid ι is to be located in the first octant of the rectangular box
Λ	affine transformation matrix of the unit sphere $\Lambda := (a,b,c)$

The notation used in the mathematical programming models is summarized in the following sections.

A.1 Indices and Sets

$d \in \{1,2,3\}$	index for the dimension; $d = 1$ represents the length and $d = 2$ the width, and $d = 3$ the height of the box
$i \in \mathcal{I} := \{1,\ldots,n\}$	objects (ellipsoids or spheres) to be packed
$(i,j) \in \mathcal{I}^{\text{co}}$	pairs of congruent ellipsoids; we assume $i < j$

A.2 Data

a_i	the largest semi-axis of ellipsoid i; $a_i \geq b_i \geq c_i$
b_i	2nd largest semi-axis of ellipsoid i; $a_i \geq b_i \geq c_i$
c_i	smallest semi-axis of ellipsoid i; $a_i \geq b_i \geq c_i$
$\overline{D}_{ij}$	bound on the distance variables d_{ij}^{ab} and d_{ij}^{be}
Δ	relative gap
R_i	radius of sphere i to be packed
S_d^-, S_d^+	minimum (lower bound) and maximum size (upper bound) of the extension of the rectangular box in dimension d
V_i	volume of ellipsoid i; $V_i = \frac{4}{3}\pi a_i b_i c_i$
V^-, V^+	lower and upper bounds on volume, v, of the rectangular box obtained during the computation
$V^{\mathrm{ci},-}$	minimal volume of the design rectangle to host the inner spheres associated with the ellipsoids. $V^{\mathrm{ci},-}$ provides a lower bound on the associated ellipsoid packing problem
$V^{\mathrm{ci},+}$	volume of the rectangular box to host the outer spheres associated with the ellipsoids. $A^{\mathrm{ci},-}$ provides an upper bound on the associated EPP
Λ_{inn}	elements of affine transformation matrix

A.3 Decision Variables

d_{ijd}^{c}	difference of the center coordinates of ellipsoid i and j
$\mathbf{n}_{ij}^{\mathrm{H}}$	normal vector of the hyperplane H_{ij} separating ellipsoid i and j; in the GAMS implementation we use n_{ijd}^{H} for each coordinate direction d subject to $-1 \leq n_{ijd}^{\mathrm{H}} \leq +1$
L_{ij}	elements of the rotation matrix L in the half-space approach; the elements are subject to the bounds $-1 \leq R_{ij} \leq +1$
R_{ij}	elements of the rotation matrix R; the elements are subject to the bounds $-1 \leq R_{ij} \leq +1$
u_{jkmn}	auxiliary variables considered only for tuples with $j \leq m$ and $k \leq n$
v	volume of the rectangular box; v^* defines (globally) optimal volume
v_i	auxiliary variable representing the trigonometric term $\cos\theta_i$; $v_i \in [-1,1]$ for ellipsoid i when using the one-axis -one angle-approach
w_i	auxiliary variable representing the trigonometric term $\sin\theta_i$; $w_i \in [0,1]$ for ellipsoid i when using the *one axis-one angle* approach
x_d^{R}	extension of the rectangular box in dimension d
x_{id}^0	coordinates of the center vector of ellipsoid i
z	waste of the rectangular box; $z = v - \sum_{i\in\mathcal{I}} V_i$
θ_i	orientation angle of ellipsoid i; $\theta_i \in [0, 2\pi]$

The model contains only continuous variables.

B Detailed Derivations

B.1 Bounds on Rotation Matrices

A rotation matrix R in real space $\mathbb{R}$ is a $n \times n$ matrix with the following properties:

$$\mathsf{R}\mathsf{R}^{\mathrm{T}} = \mathsf{R}^{\mathrm{T}}\mathsf{R} = 1\!\!1 \quad , \quad \det \mathsf{R} = +1 \quad , \tag{B.67}$$

i.e., the inverse matrix R^{-1} of R is just the transposed matrix R^{T}. From (B.67) we follow and proof that for all elements R_{ij} the following bound inequalities

$$|R_{ij}| \leq 1 \quad , \quad \forall \{ij\} \tag{B.68}$$

are true. These bounds are useful to provide them to the global solvers. The proof only exploits $\mathsf{R}^{\mathrm{T}}\mathsf{R} = 1\!\!1$ and works as follows:

$$\mathsf{R}^{\mathrm{T}}\mathsf{R} = 1\!\!1$$

is equivalent to

$$\left(\mathsf{R}^{\mathrm{T}}\mathsf{R}\right)_{ik} = \sum_j R^{\mathrm{T}}_{ij} R_{jk} = \delta_{ik} = \begin{cases} 1, & \text{if } i = k \\ 0, & \text{if } i \neq k \end{cases} \quad , \quad \forall \{ik\} \quad .$$

Therefore, using the transposed form, we also have

$$\sum_j R_{ji} R_{jk} = \delta_{ik} \quad , \quad \forall \{ik\} \quad . \tag{B.69}$$

As (B.69) must be fulfilled for all $\{ik\}$, it is especially true for $k = i$, which implies

$$\sum_j R_{ji} R_{ji} = \sum_j R^2_{ji} = \delta_{ii} = 1 \quad , \quad \forall \{i\} \quad . \tag{B.70}$$

As in (B.70) we have $\sum_j R^2_{ji} = \sum_j R^2_{ij} = 1$ for all i, it follows $|R_{ij}| \leq 1$ for all $\forall \{ij\}$. Thus, as we work in real space $\mathbb{R}$, we can add the bounds

$$-1 \leq R_{ij} \leq +1 \quad , \quad \forall \{ij\} \quad . \tag{B.71}$$

B.2 Minimal and maximal extensions of rotated ellipsoids

We compute the extreme extensions, x^-_{id} and x^+_{id}, of ellipsoid i in dimension d with center x^0_{id} from the optimization problems

$$x^-_{id} = \min\ \mathbf{c}^\top \mathbf{x} = \min\ x_{id} \quad , \quad \forall d \qquad \text{and}$$
$$x^+_{id} = \max\ \mathbf{c}^\top \mathbf{x} = \max\ x_{id} \quad , \quad \forall d \quad ,$$

subject to the ellipsoid equation (2.10); for $d = 1$ we use $\mathbf{c}^\top := (1, 0, 0)$, for $d = 2$ we select $\mathbf{c}^\top := (0, 1, 0)$, and for $d = 3$ we use $\mathbf{c}^\top := (0, 0, 1)$. Instead of using (2.10), we solve the modified and easier optimization problem

$$x^-_{id} = \min\ \mathbf{c}^\top (\mathbf{x} + \mathbf{x}^0_i) = x^0_{id} + \min\ x_{id} \quad , \quad \forall d \qquad \text{and} \tag{B.72}$$

$$x^+_{id} = \max\ \mathbf{c}^\top (\mathbf{x} + \mathbf{x}^0_i) = x^0_{id} + \max\ x_{id} \quad , \quad \forall d \quad , \tag{B.73}$$

respectively, subject to ellipsoid equation

$$\mathbf{x}^\top \mathsf{A} \mathbf{x} = 1 \quad , \tag{B.74}$$

for an origin-centered ellipsoid. Note, however, that ellipsoid i cannot be placed at the origin, the left-bottom corner of the rectangular box. Actually, a lower bound on the center coordinate, x_{id}, in all coordinate directions d is given by

$$x^0_{id} \geq c \quad , \tag{B.75}$$

if we assume that the semi-axis of ellipsoid i are sorted according to $a \geq b \geq c$.

The Lagrangian function of both optimization problems (B.72) and (B.73) reads

$$\mathcal{L}(\mathbf{x}, \bar{\lambda}) = \mathbf{c}^\top (\mathbf{x} + \mathbf{x}^0_i) + \bar{\lambda} \left(\mathbf{x}^\top \mathsf{A}_i \mathbf{x} - 1 \right) \tag{B.76}$$

with the unrestricted Lagrangian multiplier $\bar{\lambda} \in \mathbb{R}$. The first-order Karush-Kuhn-Tucker (KKT) conditions follow as

$$\mathbf{c} + 2\bar{\lambda} \mathsf{A}^\top_i \mathbf{x} = \mathbf{0} \tag{B.77}$$

together with (B.74).

We left-multiply (B.77) by $\mathbf{x}^\top$, (this operation is safe, as the origin cannot be an extremum) and exploit (B.74) to obtain $x_d + 2\bar{\lambda} = 0$ for all d. This enables us to substitute $\bar{\lambda}$ from (B.77) yielding

$$\mathbf{c} - x_d \mathsf{A}^\top \mathbf{x} = 0 \quad , \quad \forall d \quad . \tag{B.78}$$

with

$$\mathsf{A} = \begin{pmatrix} A_{11} & A_{12} & A_{13} \\ A_{21} & A_{22} & A_{23} \\ A_{31} & A_{32} & A_{33} \end{pmatrix} \quad , \quad \mathsf{A}^\top = \begin{pmatrix} A_{11} & A_{21} & A_{31} \\ A_{12} & A_{22} & A_{32} \\ A_{13} & A_{23} & A_{33} \end{pmatrix} \quad .$$

For the first dimension ($d = 1$, x-axis) the three equations in (2.32) read

$$1 - x_1 \left(A_{11} x_1 + A_{21} x_2 + A_{31} x_3 \right) = 0 \tag{B.79}$$

$$-\, x_1 \left(A_{12} x_1 + A_{22} x_2 + A_{32} x_3 \right) = 0 \tag{B.80}$$

$$-x_1 \left(A_{13} x_1 + A_{23} x_2 + A_{33} x_3 \right) = 0 \quad . \tag{B.81}$$

As $x_1 \neq 0$ (the origin cannot be a stationary point of this problem), we divide the 2nd and 3rd equation by x_1 and derive

$$\begin{aligned} 1 - x_1 \left(A_{11}x_1 + A_{21}x_2 + A_{31}x_3 \right) &= 0 \\ A_{12}x_1 + A_{22}x_2 + A_{32}x_3 &= 0 \\ A_{13}x_1 + A_{23}x_2 + A_{33}x_3 &= 0 \quad . \end{aligned} \tag{B.82}$$

At first, let us express x_2 and x_3 as functions of x_1. This leads to

$$x_2 = \frac{A_{12}A_{33} - A_{13}A_{32}}{A_{23}A_{32} - A_{22}A_{33}} x_1 \quad , \quad x_3 = \frac{A_{13}A_{22} - A_{12}A_{23}}{A_{23}A_{32} - A_{22}A_{33}} x_1 \quad . \tag{B.83}$$

If we enter the expressions (B.83) into (B.79), we obtain

$$1 - x_1^2 \left(A_{11} + A_{21} \frac{A_{12}A_{33}x - A_{13}A_{32}}{A_{23}A_{32} - A_{22}A_{33}} + A_{31} \frac{A_{13}A_{22} - A_{12}A_{23}}{A_{23}A_{32} - A_{22}A_{33}} \right) = 0 \quad ,$$

from which we further derive

$$\begin{aligned} x_1^{-2} &= \left(A_{11} + A_{21} \frac{A_{12}A_{33}x - A_{13}A_{32}}{A_{23}A_{32} - A_{22}A_{33}} + A_{31} \frac{A_{13}A_{22} - A_{12}A_{23}}{A_{23}A_{32} - A_{22}A_{33}} \right) \\ &= \frac{A_{23}A_{32} - A_{22}A_{33}}{A_{11}A_{23}A_{32} - A_{11}A_{22}A_{33} - A_{12}A_{31}A_{23} - A_{21}A_{13}A_{32} + A_{13}A_{22}A_{31} + A_{12}A_{21}A_{33}} \end{aligned}$$

and thus

$$x_1^2 = \frac{A_{22}A_{33} - A_{23}A_{32}}{\lambda_{i1}\lambda_{i2}\lambda_{i3}} = \left(A_{22}A_{33} - A_{23}A_{32} \right) a^2 b^2 c^2 \tag{B.84}$$

where we exploit the fact that

$$\begin{aligned} \det \mathsf{A} &= A_{11}A_{22}A_{33} - A_{11}A_{23}A_{32} - A_{12}A_{21}A_{33} + A_{12}A_{31}A_{23} + A_{21}A_{13}A_{32} - A_{13}A_{22}A_{31} \\ &= \lambda_{i1}\lambda_{i2}\lambda_{i3} > 0 \end{aligned}$$

(*cf.* Eigenvector Decomposition). From the geometrical background of the optimization problems (B.72) and (B.73), we know that each problem has a unique, global extremum. We further know that the global extremal values necessarily satisfy the KKT conditions (B.74) and (B.77). Because we have not excluded any global optima in our derivation to obtain (B.84) which leads to exactly two points, we know that x_1 in (B.84) gives the global optimum for (B.73) and (B.72); we just need to select the proper one.

The minimal and maximal extensions of the ellipsoid in the first dimension, ($d = 1$), then reduce to

$$x_1^- = \min \ \mathbf{c}^\top (\mathbf{x} + \mathbf{x}^0) = x_1^0 - \sqrt{x_1^2} = x_1^0 - abc\sqrt{A_{22}A_{33} - A_{23}A_{32}} \tag{B.85}$$

and

$$x_1^+ = x_1^0 + abc\sqrt{A_{22}A_{33} - A_{23}A_{32}} \quad , \tag{B.86}$$

respectively. Note that these formulae are similar to (18) and (19) in KR14 obtained for the maximal extensions of ellipses (2D case). If the ellipsoids were spheres ($a = b = c = r$), for $\theta_1 = \theta_2 = \theta_3 = 0$, we obtain $x_1^+ = x_1^0 + abc\sqrt{b^{-2}c^{-2} - 0} = x_1^0 + r$.

Similarly, for $d = 2$ we derive

$$-x_2 \left(A_{11}x_1 + A_{21}x_2 + A_{31}x_3 \right) = 0 \tag{B.87}$$

$$1 - x_2 \left(A_{12}x_1 + A_{22}x_2 + A_{32}x_3 \right) = 0 \tag{B.88}$$

$$-x_2 \left(A_{13}x_1 + A_{23}x_2 + A_{33}x_3 \right) = 0 \quad . \tag{B.89}$$

At first, let us express x_1 and x_3 as functions of x_2. This leads to

$$x_1 = \frac{A_{21}A_{33} - A_{31}A_{23}}{A_{13}A_{31} - A_{11}A_{33}} x_2 \quad , \quad x_3 = \frac{A_{11}A_{23} - A_{21}A_{13}}{A_{13}A_{31} - A_{11}A_{33}} x_2 \quad . \tag{B.90}$$

If we enter the expressions (B.83) into (B.79), we obtain

$$1 - x_2^2 \left(A_{12} \frac{A_{21}A_{33} - A_{31}A_{23}}{A_{13}A_{31} - A_{11}A_{33}} + A_{22} + A_{32} \frac{A_{11}A_{23} - A_{21}A_{13}}{A_{13}A_{31} - A_{11}A_{33}} \right) = 0 \quad ,$$

from which we further derive

$$
\begin{aligned}
x_1^2 &= \left(A_{12}\frac{A_{21}A_{33} - A_{31}A_{23}}{A_{13}A_{31} - A_{11}A_{33}} + A_{22} + A_{32}\frac{A_{11}A_{23} - A_{21}A_{13}}{A_{13}A_{31} - A_{11}A_{33}} \right)^{-1} \\
&= (A_{13}A_{31} - A_{11}A_{33})\,(\det \mathsf{A})^{-1}
\end{aligned}
$$

and thus

$$
x_2^2 = \frac{A_{11}A_{33} - A_{13}A_{31}}{\lambda_{i1}\lambda_{i2}\lambda_{i3}} = a^2b^2c^2\,(A_{11}A_{33} - A_{13}A_{31}) \quad ,
$$

which finally leads to

$$
x_2^- = x_2^0 - abc\sqrt{A_{11}A_{33} - A_{13}A_{31}} \tag{B.91}
$$

$$
x_2^+ = x_2^0 + abc\sqrt{A_{11}A_{33} - A_{13}A_{31}} \quad . \tag{B.92}
$$

Similarly, for $d = 3$ we derive

$$
-x_3\,(A_{11}x_1 + A_{21}x_2 + A_{31}x_3) = 0 \tag{B.93}
$$

$$
-\,x_3\,(A_{12}x_1 + A_{22}x_2 + A_{32}x_3) = 0 \tag{B.94}
$$

$$
1 - x_3\,(A_{13}x_1 + A_{23}x_2 + A_{33}x_3) = 0 \quad . \tag{B.95}
$$

$$
\begin{aligned}
(A_{11}x_1 + A_{21}x_2 + A_{31}x_3) &= 0 \\
(A_{12}x_1 + A_{22}x_2 + A_{32}x_3) &= 0
\end{aligned}
$$

At first, let us express x_1 and x_2 as functions of x_3. This leads to

$$
x_1 = \frac{A_{22}A_{31} - A_{21}A_{32}}{A_{12}A_{21} - A_{11}A_{22}}x_3 \quad , \quad x_2 = \frac{A_{11}A_{32} - A_{12}A_{31}}{A_{12}A_{21} - A_{11}A_{22}}x_3 \quad . \tag{B.96}
$$

If we enter the expressions (B.96) into (B.95), we obtain

$$
A_{13}\frac{A_{22}A_{31} - A_{21}A_{32}}{A_{12}A_{21} - A_{11}A_{22}} + A_{23}\frac{A_{11}A_{32} - A_{12}A_{31}}{A_{12}A_{21} - A_{11}A_{22}} + A_{33}x_3
$$

$$
1 - x_3^2\left(A_{13}\frac{A_{22}A_{31} - A_{21}A_{32}}{A_{12}A_{21} - A_{11}A_{22}} + A_{23}\frac{A_{11}A_{32} - A_{12}A_{31}}{A_{12}A_{21} - A_{11}A_{22}} + A_{33} \right) = 0 \quad ,
$$

from which we further derive

$$
\begin{aligned}
x_3^2 &= \left(A_{13}\frac{A_{22}A_{31} - A_{21}A_{32}}{A_{12}A_{21} - A_{11}A_{22}} + A_{23}\frac{A_{11}A_{32} - A_{12}A_{31}}{A_{12}A_{21} - A_{11}A_{22}} + A_{33} \right)^{-1} \\
&= (A_{12}A_{21} - A_{11}A_{22})\,(\det \mathsf{A})^{-1}
\end{aligned}
$$

and thus

$$
x_3^2 = \frac{A_{11}A_{22} - A_{12}A_{21}}{\lambda_{i1}\lambda_{i2}\lambda_{i3}} = a^2b^2c^2\,(A_{11}A_{22} - A_{12}A_{21}) \quad .
$$

Therefore, the minimal and maximal extensions of ellipsoid i in the third dimension, ($d = 3$), reduce to

$$
x_3^- = \min\ \mathbf{c}^\top(\mathbf{x} + \mathbf{x}^0) = x_3^0 - \sqrt{x_3^2} = x_3^0 - abc\sqrt{A_{11}A_{22} - A_{12}A_{21}} \tag{B.97}
$$

and

$$
x_3^+ = x_3^0 + abc\sqrt{A_{11}A_{22} - A_{12}A_{21}} \quad , \tag{B.98}
$$

respectively.

B.3 Inner Rectangular Box

Inner rectangular boxes can be computed by maximizing the first octant volume xyz (later we multiply this by 2^3) subject to the condition that the point (x, y, z) is on the ellipsoid and fulfills the equality

$$\frac{x^2}{a^2} + \frac{y^2}{b^2} + \frac{z^2}{c^2} = 1 \quad .$$

The Lagrangian function is

$$xyz - \lambda \left[\frac{x^2}{a^2} + \frac{y^2}{b^2} + \frac{z^2}{c^2} - 1 \right] \quad .$$

The KKT are

$$\begin{aligned} yza^2 - 2\lambda x &= 0 \\ xzb^2 - 2\lambda y &= 0 \\ xyc^2 - 2\lambda z &= 0 \quad . \end{aligned}$$

Multiplication by y and x of the first, and z and y of the second and third equation, gives

$$\begin{aligned} y^2za^2 - 2\lambda xy &= 0 \\ x^2zb^2 - 2\lambda xy &= 0 \end{aligned}$$

and

$$\begin{aligned} xz^2b^2 - 2\lambda yz &= 0 \\ xy^2c^2 - 2\lambda yz &= 0 \end{aligned}$$

which can be reduced to

$$\begin{aligned} y^2za^2 - x^2zb^2 &= 0 = y^2a^2 - x^2b^2 \\ xz^2b^2 - xy^2c^2 &= 0 = z^2b^2 - y^2c^2 \quad , \end{aligned}$$

where we have exploited that $z \neq 0$ and $x \neq 0$. That implies

$$\frac{x^2}{a^2} = \frac{y^2}{b^2} = \frac{z^2}{c^2} \quad .$$

Together with

$$\frac{x^2}{a^2} + \frac{y^2}{b^2} + \frac{z^2}{c^2} = 1$$

we thus obtain

$$\frac{x^2}{a^2} = \frac{y^2}{b^2} = \frac{z^2}{c^2} = \frac{1}{3}$$

or

$$x = \frac{1}{\sqrt{3}}a \approx 0.58a \quad , \quad y = \frac{1}{\sqrt{3}}b \approx 0.58b \quad , \quad z = \frac{1}{\sqrt{3}}c \approx 0.58c \quad ,$$

and the volume maximal volume of the complete rectangular box is

$$v = 2^3 \left(\frac{\sqrt{3}}{3}a \right) \left(\frac{\sqrt{3}}{3}b \right) \left(\frac{\sqrt{3}}{3}c \right) = \sqrt{3}\frac{8}{9}abc \approx 1.54abc < \pi abc$$

which is approximately half the volume πabc of the ellipsoid.

B.4 Plotting ellipsoids

Knowing the rotation-shape matrix A and the origin $\mathbf{x}^0$, we exploit the ellipsoid equation

$$\mathbf{x}^\top \begin{pmatrix} A_{11} & A_{21} & A_{31} \\ A_{12} & A_{22} & A_{32} \\ A_{13} & A_{23} & A_{33} \end{pmatrix} \mathbf{x} = 1$$

to obtain $\mathbf{x}^\top = (x, y, z)$ and plot the ellipsoid.

$$(x, y, z) \begin{pmatrix} A_{11} & A_{21} & A_{31} \\ A_{21} & A_{22} & A_{32} \\ A_{31} & A_{32} & A_{33} \end{pmatrix} \begin{pmatrix} x \\ y \\ z \end{pmatrix} = 1$$

leads to

$$x^2 A_{11} + y^2 A_{22} + z^2 A_{33} + 2xyA_{21} + 2xzA_{31} + 2yzA_{32} = 1 \quad . \tag{B.99}$$

If we introduce spherical coordinates (θ,φ) with $-\pi/2 \le \theta \le \pi/2$ and $0 \le \varphi \le 2\pi$ we get

$$\begin{pmatrix} X \\ Y \\ Z \end{pmatrix} = \begin{pmatrix} \cos\theta\cos\varphi \\ \cos\theta sin\varphi \\ \sin\theta \end{pmatrix}$$

for the coordinates of a point (X, Y, Z) on the unit sphere, *resp.*,

$$\begin{aligned} X &= X(\theta, \varphi) = \cos\theta\cos\varphi \\ Y &= Y(\theta, \varphi) = \cos\theta\sin\varphi \\ Z &= Z(\theta, \varphi) = \sin\theta \quad . \end{aligned}$$

Finally, with the scaling function $\rho = \rho(\theta, \varphi)$ we obtain the ellipsoid points

$$\begin{pmatrix} x' \\ y' \\ z' \end{pmatrix} = \rho \begin{pmatrix} X \\ Y \\ Z \end{pmatrix}$$

and from (B.99)

$$\rho^2 = \frac{1}{X^2 A_{11} + Y^2 A_{22} + Z^2 A_{33} + 2XYA_{21} + 2XZA_{31} + 2YZA_{32}} \quad .$$

Note that ρ is the extension of the ellipsoid measured from the center of the ellipsoid in the direction of (θ, φ). Thus, it is always positive and bounded by $c \le \rho \le a$, if we assume that $a \ge b \ge c$.

Considering the origin $\mathbf{x}^0$, we obtain the parametric representation of the ellipsoid

$$\mathbf{x} = \mathbf{x}(\theta, \varphi) = \begin{pmatrix} x \\ y \\ z \end{pmatrix} = \begin{pmatrix} x^0 \\ y^0 \\ z^0 \end{pmatrix} + \rho \begin{pmatrix} X \\ Y \\ Z \end{pmatrix} \quad .$$

References

1. Cafieri, S., Lee, J., Liberti, L.: On convex relaxations of quadrilinear terms (2009). DOI 10.1007/s10898-009-9484-1
2. Chernov, N., Stoyan, Y., Romanova, T., Pankratov, A.: Phi-Functions for 2D Objects Formed by Line Segments and Circular Arcs. Advances in Operations Research (2012). DOI 10.1155/2012/346358
3. Choi, Y.K., Chang, J.W., Wang, W., Kim, M.S., Elber, G.: Continuous Collision Detection for Ellipsoids. IEEE Transactions on Visualization & Computer Graphics **15(2)**, 311–325 (2009). DOI 10.1109/TVCG.2008.80
4. Dirac, P.A.M.: The Principles of Quantum Mechanics. Oxford University Press, Oxford, UK (1974)
5. Donev, A., Cisse, I., Sachs, D., Variano, E.A., Stillinger, F.H., Connelly, R., Torquato, S., Chaikin, P.M.: Improving the Density of Jammed Disordered Packings Using Ellipsoids. Science **303**(5660), 990–993 (2004). DOI 10.1126/science.1093010. URL http://dx.doi.org/10.1126/science.1093010
6. Donev, A., Stillinger, F.H., Chaikin, P.M., , Torquato, S.: Unusually Dense Crystal Packings of Ellipsoids. Physical Review Letters **92**, 255,506 (2004)

7. Halmos, P.R.: Finite-Dimensional Vector Spaces. Springer, New York (1974)
8. Kallrath, J.: Combined Strategic Design *and* Operative Planning in the Process Industry. Computers and Chemical Engineering **33**, 1983–1993 (2009)
9. Kallrath, J.: Cutting Circles and Polygons from Area-Minimizing Rectangles. Journal of Global Optimization **43**, 299–328 (2009)
10. Kallrath, J.: Polylithic Modeling and Solution Approaches Using Algebraic Modeling Systems. Optimization Letters **5**, 453–466 (2011). 10.1007/s11590-011-0320-4
11. Kallrath, J., Rebennack, S.: Cutting Ellipses from Area-Minimizing Rectangles. Journal of Global Optimization **59(2-3)**, 405–437 (2014). DOI 10.1007/s10898-013-0125-3
12. Lindo Systems: Lindo API: User's Manual. Lindo Systems, Inc., Chicago (2004)
13. Lubachevsky, B.D., Stillinger, F.H.: Geometric properties of random disk packings. Journal of Statistical Physics **60(5-6)**, 561–583 (1990)
14. Man, W., Donev, A., Stillinger, F.H., Sullivan, M.T., Russel, W.B., Heeger, D., Inati, S., Torquato, S., Chaikin, P.M.: Experiments on random packings of ellipsoids. Phys. Rev. Lett. **94**, 198,001 (2005). DOI 10.1103/PhysRevLett.94.198001. URL http://link.aps.org/doi/10.1103/PhysRevLett.94.198001
15. Misener, R., Floudas, C.: ANTIGONE: Algorithms for coNTinuous / Integer Global Optimization of Nonlinear Equations. Journal of Global Optimization **59**, 503–526 (2014). DOI 10.1007/s10898-014-0166-2
16. Romanova, T., Scheithauer, G., Krivulya, A.: Covering a polygonal region by rectangles. Computational Optimization and Applications **48(3)**, 675–695 (2011)
17. Stoyan, Y.G., Chugay, A.: Packing cylinders and rectangular parallelepipeds with distances between them. European Journal of Operational Research **197(1)**, 446–455 (2008)
18. Tawarmalani, M., Sahinidis, N.V.: Convexification and Global Optimization in Continuous and Mixed-Integer Nonlinear Programming: Theory, Algorithms, Software, and Applications. Nonconvex Optimization And Its Applications Series. Kluwer Academic Publishers, Dordrecht, The Netherlands (2002)
19. Uhler, C., Wright, S.J.: Packing ellipsoids with overlap. SIAM Review **55**(4), 671–706 (2013). DOI 10.1137/120872309. URL http://dx.doi.org/10.1137/120872309
20. Waldron, K., Schmiedeler, J.: Kinematics. In: B. Siciliano, O. Khatib (eds.) Handbook of Robotics, pp. 9–33. Springer, Oxford, UK (2008)